JOC The Journal of Organic Chemistry

Article

pubs.acs.org/joc

Synthesis, Structure, and Characterization of Chromo(fluoro)ionophores with Cation-Triggered Emission Based on *N*-Methylaza-Crown-Ether Styryl Dyes

Sergey P. Gromov,*[,†] Svetlana N. Dmitrieva,[†] Artem I. Vedernikov,[†] Nikolay A. Kurchavov,[†] Lyudmila G. Kuz'mina,[‡] Sergey K. Sazonov,[†] Yuri A. Strelenko,[§] Michael V. Alfimov,[†] Judith A. K. Howard,[∥] and Evgeny N. Ushakov[⊥]

[†]Photochemistry Center, Russian Academy of Sciences, ul. Novatorov 7A-1, Moscow 119421, Russian Federation

[‡]N. S. Kurnakov Institute of General and Inorganic Chemistry, Russian Academy of Sciences, Leninskiy prosp. 31, Moscow 119991, Russian Federation

[§]N. D. Zelinskiy Institute of Organic Chemistry, Russian Academy of Sciences, Leninskiy prosp. 47, Moscow 119991, Rusian Federation

[∥]Chemistry Department, Durham University, South Road, Durham DH1 3LE, United Kingdom

[⊥]Institute of Problems of Chemical Physics, Russian Academy of Sciences, prosp. Akad. Semenova 1, Chernogolovka 142432, Moscow Region, Russian Federation

Supporting Information

ABSTRACT: Novel 2-benzothiazole-, 4-pyridine-, and 2- and 4-quinoline-based styryl dyes containing an *N*-methylbenzoaza-15(18)-crown-5(6)-ether moiety were synthesized. A detailed electronic spectroscopy study revealed high performance of these compounds as optical molecular sensors for alkali and alkaline-earth metal cations. They were shown to considerably surpass analogous chromoionophores based on *N*-phenylaza-crown ethers regarding both the ionochromism and the cation-binding ability. In addition, they act as fluorescent sensors for the metal cations by demonstrating cation-triggered emission. Upon complexation with Ba^{2+}, the fluorescence enhancement factor reaches 61. The structural features of dyes and their metal complexes were studied by NMR spectroscopy and X-ray diffraction. The high degree of macrocycle preorganization was found to be one of the factors determining the high cation-binding ability of the sensor molecules based on *N*-methylbenzoaza-crown ethers.

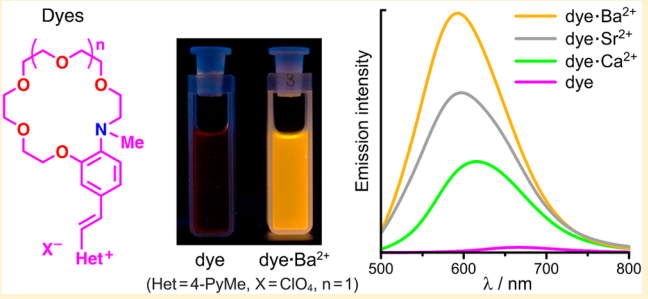

INTRODUCTION

Currently, a topical problem is the development of selective and sensitive sensors for analytical applications in chemistry, biology, medicine, ecology, and other fields. In this connection, of considerable interest are chromogenic and luminogenic crown compounds (chromo- and fluoroionophores) able to change their photophysical properties considerably upon selective binding of a substrate.[1] They are expected to find use in portable optical devices for determination of metal cations and some organic cations. The design of intrinsic chromo(fluoro)ionophores based on electron-coupled donor−acceptor systems often makes use of *N*-phenylaza-crown-ether moieties,[1,2] as they have good electron-donating properties. A substantial drawback of the chromogenic *N*-phenylaza-crown ethers is low thermodynamic stability of the complexes with alkali and alkaline-earth metal cations compared with benzo-crown-ether-based analogues.[3] In addition, an increase in the electron-withdrawing ability of the moiety conjugated to the crown ether does not always result in the expected enhancement of the cation-induced optical signal but may conversely attenuate the signal.[4] We suggested that these problems can be resolved by using 1-aza-2,3-benzo-crown ethers instead of *N*-phenylaza-crown ethers. Previously, we studied a large series of benzoaza-crown ethers in which we varied a number of structural parameters: the macrocycle size, the number and position of the nitrogen atoms in the macrocycle, and also substituents in the benzene ring and at nitrogen atoms.[5] It was shown by X-ray diffraction analysis and NMR spectroscopy that *N*-alkyl derivatives of benzoaza-crown ethers in which nitrogen is directly connected to the benzene ring are preorganized for the formation of complexes with metal and ammonium cations. A comparative study of complexing properties showed that *N*-methyl derivatives are preferable among them as regards the ion-binding ability and selectivity toward alkali and alkaline-earth cations.

Received: July 17, 2013
Published: September 3, 2013

This paper presents the synthesis of 2-benzothiazole-, 2- and 4-quinoline-, and 4-pyridine-derived styryl dyes **1**–**5** containing the most promising *N*-methylbenzoaza-crown-ether moiety. Styryl dye **6** containing an *N*-phenylaza-18-crown-6-ether moiety, and being a structural analogue of compound **1b**, was synthesized to be used as the reference chromoionophore. The effect of complexation with alkali and alkaline-earth metal cations on the photophysical and photochemical properties of the obtained dyes was studied by electronic spectroscopy. The structural features of dyes and their metal complexes were investigated by NMR spectroscopy and X-ray diffraction analysis.

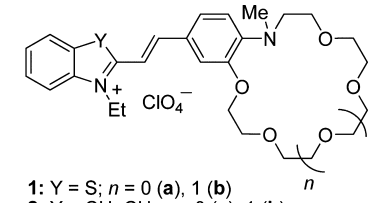

1: Y = S; *n* = 0 (**a**), 1 (**b**)
2: Y = CH=CH, *n* = 0 (**a**), 1 (**b**)

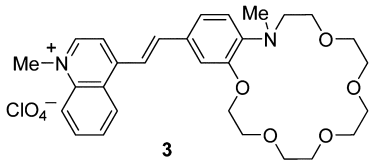

3

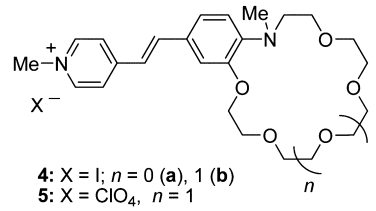

4: X = I; *n* = 0 (**a**), 1 (**b**)
5: X = ClO_4, *n* = 1

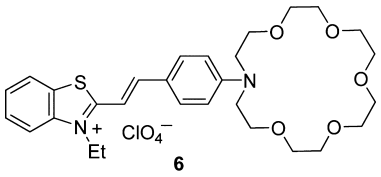

6

RESULTS AND DISCUSSION

Synthesis of Dyes 1–6. Dyes **1**–**5** were prepared in high yields (up to 89%) by condensation of *N*-methyl-(formylbenzo)aza-15(18)-crown-5(6) ethers **7a,b**[5a,c] with quaternary salts of heterocyclic bases **8**–**12** in the presence of an organic base (pyridine in the case of **1** and pyrrolidine or piperidine in other cases) in ethanol or methanol (Scheme 1). The yields of dyes with 15-membered macrocycles were somewhat higher than the yields of dyes with 18-membered macrocycles, probably due to lower solubility of the former in the reaction medium.

Dye **6** was prepared in a 69% yield by condensation of *N*-(formylphenyl)aza-18-crown-6 ether **13**[6] with quaternary salt **8** (Scheme 2), similarly to the procedure described previously.[7]

The structures of all of the obtained compounds were determined by ^{1}H and ^{13}C NMR spectroscopy and confirmed by elemental analysis data (^{1}H and ^{13}C NMR spectra and two-dimensional correlation spectroscopy (2D COSY), nuclear Overhauser effect spectroscopy (NOESY), heteronuclear single quantum coherence spectroscopy (HSQC), and heteronuclear multiple-bond correlation spectroscopy (HMBC) spectra of dyes **1**–**6** are shown in Figures S1–S53 in the Supporting Information to this article). All dyes have the *E* configuration of the ethylene bond, judging by the spin–spin coupling constant $^3J_{HC=CH}$ = 15.3–16.4 Hz.

Scheme 1. Synthesis of Dyes 1–5

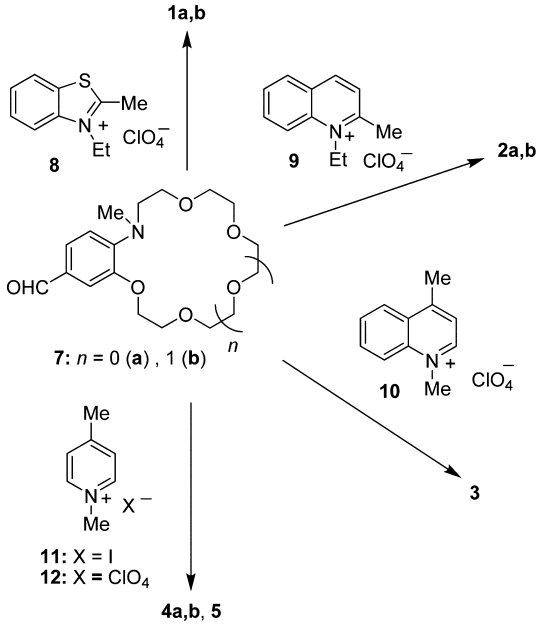

Scheme 2. Synthesis of Dye 6

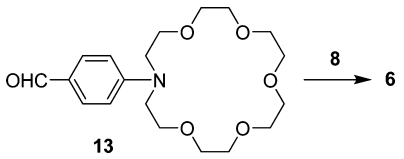

Electronic Spectroscopy Study. The complexation of dyes **1a,b**, **2b**, **3**, **5**, and **6** with alkali and alkaline-earth metal cations in MeCN was studied by spectrophotometric titration (see the Experimental Section and Figures S54–S59 in the Supporting Information). The spectroscopic data were treated using global analysis methods.[8] Table 1 gives the key absorption and fluorescence characteristics of dyes and their complexes. The complex stability constants are summarized in Table 2.

In all cases, the complex formation induces a hypsochromic shift of the long-wavelength absorption band of the dye ($\Delta\lambda$). Dyes **1**–**6** are donor–acceptor type chromoionophores,[1a,f] and the observed hypsochromic shifts are due to the interaction between the complexed metal cation and the heteroatoms of the electron-donating part of the chromophore. The coordination bond between the metal cation and the macrocyclic nitrogen atom incorporated in the conjugated π-electron system of the styryl dye has a crucial effect on the $\Delta\lambda$ value. The $\Delta\lambda$ value for the complexes of alkaline-earth cations with the benzoaza-15-crown-5 derivative **1a** and benzoaza-18-crown-6 derivatives **1b**, **2b**, **3**, and **5** increases with a decrease in the metal cation diameter (d_M). In other words, the strength of the coordination bond N···M^{2+} increases with the increase in the cation charge density.

No general correlation between $\Delta\lambda$ and d_M was found for complexes with alkali metal cations. In this case, the magnitude

dx.doi.org/10.1021/jo401555a | J. Org. Chem. 2013, 78, 9834–9847

Table 1. Electronic Absorption and Emission Spectroscopy Data for Dyes 1a,b, 2b, 3, 5, and 6; Their 1:1 Complexes with Metal Cations and Protonated Dye 1a[a]

compound	λ_{max}/nm	$\varepsilon_{max} \times 10^{-4}/M^{-1}\ cm^{-1}$	$\Delta\lambda$/nm	λ^{f}_{max}/nm	$S \times 10^{-3}/cm^{-1}$	φ_f
1a	518	4.20		642	3.7	0.0026
1a·H^+	367	3.12	151	456	5.3	0.014
1a·Li^+	413	3.22	105	621	8.1	0.013
1a·Na^+	423	3.20	95	629	7.7	0.0097
1a·Mg^{2+}	382	3.42	136	496	6.0	0.011
1a·Ca^{2+}	395	3.47	123	599	8.8	0.033
1a·Sr^{2+}	405	3.50	113	598	8.0	0.039
1a·Ba^{2+}	410	3.44	108	610	8.0	0.026
1b	526	4.30		643	3.5	0.0027
1b·Li^+	508[b]	3.38	18			
1b·Na^+	443	3.17	83	638	6.9	0.021
1b·K^+	441	3.37	85			
1b·Ca^{2+}	399	3.46	127	606	8.6	0.027
1b·Sr^{2+}	401	3.44	125	591	8.0	0.054
1b·Ba^{2+}	409	3.43	117	592	7.6	0.070
2b	512	3.20				$<10^{-3}$
2b·Li^+	498[b]	2.21	14			
2b·Na^+	434	2.74	78			
2b·K^+	433	2.91	79			
2b·Ca^{2+}	395	3.24	117	656	10.1	0.0044
2b·Sr^{2+}	397	3.23	115	628	9.3	0.0087
2b·Ba^{2+}	404	3.20	108	637	9.1	0.0090
3	519	2.60				$<10^{-3}$
3·Li^+	421[c]	1.63	88			
3·Na^+	443	2.44	76			
3·K^+	442.5	2.50	76.5			
3·Ca^{2+}	404	2.73	115	692	10.3	0.011
3·Sr^{2+}	405	2.76	114	672	9.8	0.020
3·Ba^{2+}	413	2.75	106	671	9.3	0.026
5	459	2.80		666	6.8	0.0018
5·Li^+	377[c]	1.77	82			
5·Na^+	401	2.65	58			
5·K^+	401	2.72	58			
5·Ca^{2+}	367	3.05	92	615	11.0	0.041
5·Sr^{2+}	369	3.06	90	598	10.4	0.080
5·Ba^{2+}	376	3.02	83	594	9.8	0.11
6	525	7.00				
6·Li^+	516	6.29	9			
6·Na^+	516	6.46	9			
6·K^+	504	5.57	21			
6·Ca^{2+}	497	5.01	28			
6·Sr^{2+}	402[c]	3.26	123			
6·Ba^{2+}	400[c]	3.21	125			

[a]In MeCN (water content < 0.03% v/v) at 23 ± 2 °C; counterions ClO_4^-; λ_{max} is the long-wavelength absorption maximum; ε_{max} is the molar absorption coefficient at λ_{max}; $\Delta\lambda = \lambda_{max}$(free dye) − λ_{max}(complex); λ^{f}_{max} is the maximum in the corrected fluorescence spectrum; S is the Stokes shift; φ_f is the fluorescence quantum yield. [b]The band exhibits a short-wavelength shoulder. [c]The band exhibits a long-wavelength shoulder.

of $\Delta\lambda$ and, hence, the strength of the coordination bond N···M^+ is substantially affected by the macrocyclic factor (i.e., the degree of compliance between the cation diameter and the size of the macrocycle cavity). One manifestation of the macrocyclic factor is the inverse pattern of the dependences of $\Delta\lambda$ on d_M for complexes of **1a,b** with Li^+ and Na^+.

The nature of the heterocyclic residue has a moderate influence on the complexing ability of aza-crown dyes: the stability constants for the complexes of benzoaza-18-crown-6 derivatives with alkali and alkaline-earth metal cations increase in the series of dyes with 2-benzothiazole (**1b**) < 2-quinoline (**2b**) < 4-quinoline (**3**) < 4-pyridine (**5**) residues. The ionochromic effect $\Delta\lambda$ decreases in this sequence except for the Li^+ complexes, which show two-band absorption spectra (Figure 1).

The short-wavelength band in the spectra of **1b**·Li^+ and **2b**·Li^+ has a rather low intensity and shows itself as a shoulder of the main absorption band, whereas in the spectra of **3**·Li^+ and **5**·Li^+, the short-wavelength band predominates. The intensity ratio of two bands varies in parallel with the complex stability constant (i.e., it increases in the sequence of dyes containing 2-benzothiazole (**1b**) < 2-quinoline (**2b**) < 4-quinoline (**3**) < 4-pyridine (**5**) residues).

dx.doi.org/10.1021/jo401555a | J. Org. Chem. 2013, 78, 9834−9847

Table 2. Stability Constants for the 1:1 Complexes of Dyes 1a,b, 2b, 3, 5, and 6 with Metal Cations As Measured by Spectrophotometry[a]

	log *K*						
compound	Li^+	Na^+	K^+	Mg^{2+}	Ca^{2+}	Sr^{2+}	Ba^{2+}
1a	3.12	2.72		5.30	5.24	4.71	4.24
1b	2.30	3.53	3.78	<2	7.19	8.03	7.60
2b	2.50	3.87	4.11	<2	7.67	8.37	8.08
3	2.53	3.96	4.25	<2	7.86	8.54	8.21
5	2.58	4.01	4.29	<2	7.94	8.72	8.29
6	1.80	3.03			5.17	4.94	4.81

[a]In MeCN (water content < 0.03% v/v) at 23 ± 2 °C; ionic strength 0.01 M; counterions ClO_4^-; the *K* values are measured to within about ±10% (alkali cations) or ±20% (alkaline-earth cations).

These observations suggest that Li^+ complexes of benzoaza-18-crown-6-ether derivatives **1b**, **2b**, **3**, and **5** exist as two equilibrated conformations **A** and **B** (Scheme 3). Conformers **B** in which the coordination bond N···Li^+ is disrupted are responsible for the long-wavelength bands in the spectra of the complexes. Most likely, in these conformers, the bond between Li^+ and the oxygen atom connected directly to the benzene ring is also disrupted (this assumption is based on X-ray diffraction data for complex **2b**·Li^+, see below). The observed equilibrium is due to the fact that the aza-18-crown-6-ether cavity is too large for the lithium cation. The shortage of the coordination bonds between Li^+ and the macrocycle heteroatoms in conformers **B** may be compensated for by inclusion of a solvent molecule in the first coordination sphere of lithium and by decrease in the conformational energy of the macrocycle. Note that we hypothesized the coexistence of type **A** and **B** conformers for the complexes of *N*-phenylaza-crown-ether analogues of dye **1a**;[3b] however, no direct evidence has yet been found.

The Li^+ complex of benzoaza-15-crown-5-ether derivative **1a** shows an exceptionally strong hypsochromic shift ($\Delta\lambda$ = 105 nm) and, judging by the absorption spectrum (Figure 2), it has only one conformation of type **A** in which the metal cation is coordinated to the macrocycle nitrogen.

Conversely, judging by the very small $\Delta\lambda$ = 9 nm and the shape of the spectrum (Figure 3), the Li^+ complex of the phenylaza-18-crown-6-ether derivative **6** exists only as conformations with disrupted N···Li^+ bonds. Moreover, the N···M^{m+} bond is also disrupted in the complexes of **6** with Na^+, K^+, and Ca^{2+}; as a consequence, the ionochromic effects with these cations are much less pronounced than those for related benzoaza-18-crown-6-ether derivative **1b**.

Benzoaza-crown-ether derivative **1b** also substantially surpasses **6** in the complexing ability. The most pronounced differences are observed for doubly charged cations; for example, the stability constant of **1b**·Sr^{2+} is 3 orders of magnitude greater than that for **6**·Sr^{2+}. These differences are attributable to two factors. Most important is apparently the higher electron-donating ability of the macrocyclic nitrogen in **1b** than in dye **6**. The other factor is that benzoaza-crown-ether moiety is better preorganized toward complexation than the phenylaza-crown-ether moiety. It is also noteworthy that regarding the complexing ability, benzoaza-crown-ether derivatives **1a**,**b** do not differ considerably from the related dyes based on benzo-crown ethers.[1f]

Styryl dyes **1a**,**b**, **2b**, **3**, and **5** have very low fluorescence quantum yields ($\varphi_f \sim 10^{-3}$ or less). The complexation with metal cations results in fluorescence enhancement. The fluorescence enhancement factors (FEF) for the complexes of benzoaza-18-crown-6 ethers **1b**, **2b**, **3**, and **5** with alkaline-earth metal cations increase with increase in d_M. The cation-induced shifts of the fluorescence spectra of **1b**, **2b**, **3**, and **5** are much smaller on the energy scale than the shifts of the absorption spectra (see Figure 4 for **5**, and Figures S60 and S61 in the Supporting Information) (i.e., complex formation leads to an increase in the Stokes shift). The magnitude of the Stokes shift increases in the sequence $Ba^{2+} < Sr^{2+} < Ca^{2+}$ to reach 11 000 cm^{-1} for **5**·Ca^{2+}.

The increase in the Stokes shift upon the complexation is typical of intrinsic fluoroionophores based on aza-crown ethers.

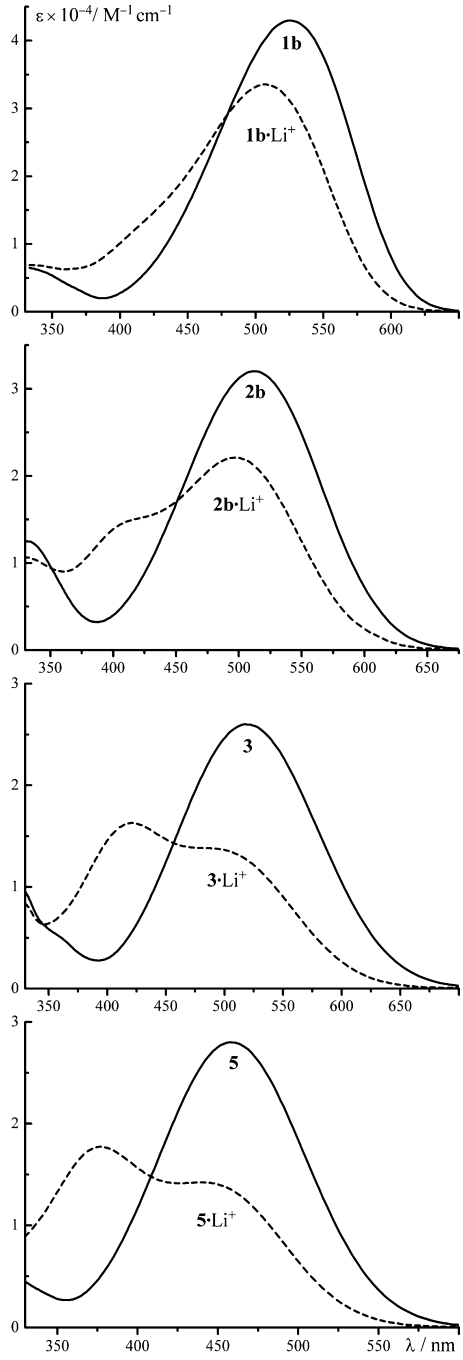

Figure 1. Absorption spectra of dyes **1b**, **2b**, **3**, and **5** and their 1:1 complexes with Li^+ in MeCN.

dx.doi.org/10.1021/jo401555a | J. Org. Chem. 2013, 78, 9834−9847

Scheme 3. Conformational Equilibrium for Complex 5·Li$^+$ in the Ground State

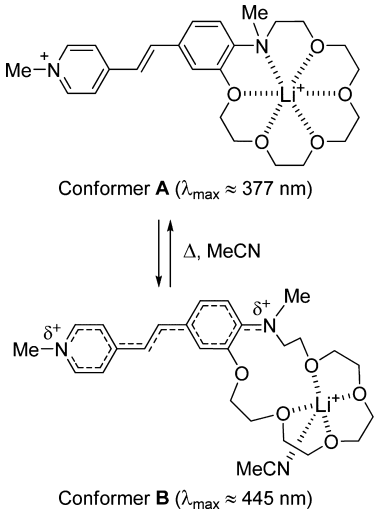

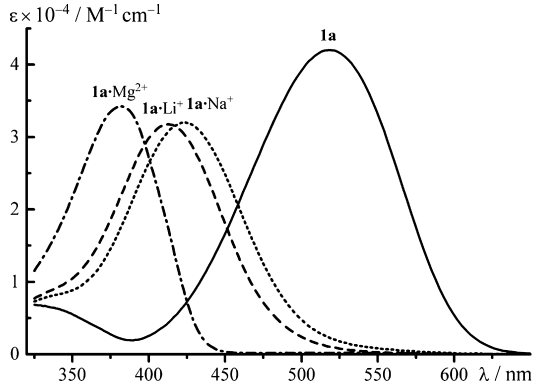

Figure 2. Absorption spectra of dye **1a** and its 1:1 complexes with Li$^+$, Na$^+$, and Mg^{2+} in MeCN.

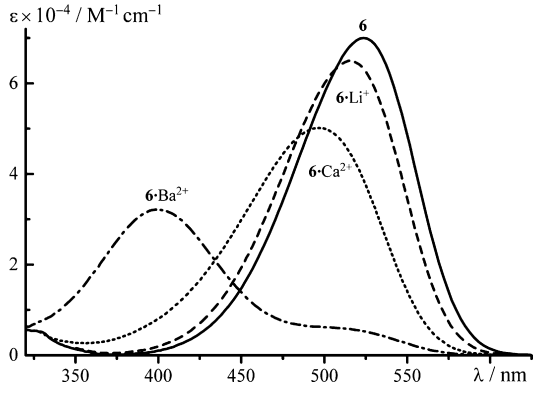

Figure 3. Absorption spectra of dye **6** and its 1:1 complexes with Li$^+$, Ca^{2+}, and Ba^{2+} in MeCN.

This can be attributed to the fact that the charge-transfer electronic transition in the fluorophore induces re-coordination of the metal cation in the aza-crown-ether cavity; this is accompanied by an increase in the distance between the cation and the nitrogen atom (i.e., the N···M^{m+} bond is either weakened or broken).[3b,4] Due to the fast re-coordination, the major contribution to the fluorescence spectra of the complexes is made by the excited states with the disrupted N···M^{m+} bond. This bond may be elongated to a higher extent in Ca^{2+}

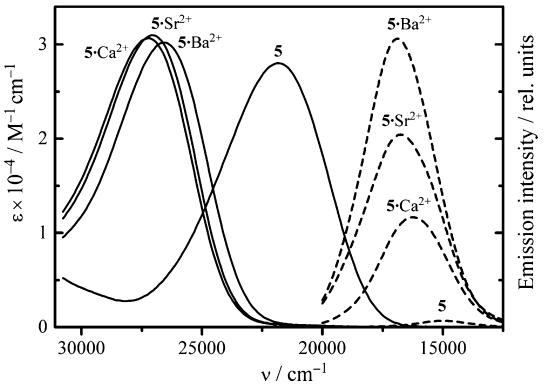

Figure 4. Absorption spectra (solid curves) and corrected emission spectra (dashed curves) of dye **5** and complexes **5**·Ca^{2+}, **5**·Sr^{2+}, and **5**·Ba^{2+} in MeCN. The emission spectra are normalized so that the integral intensities are directly proportional to the fluorescence quantum yields.

complexes than in the Sr^{2+} or Ba^{2+} complexes of **1b**, **2b**, **3**, and **5**, as the diameter of the calcium cation is smaller than the benzoaza-18-crown-6-ether cavity. Therefore, the influence of the complexation on the fluorescence spectra of these dyes is less pronounced in the case of Ca^{2+} than in the case of Sr^{2+} or Ba^{2+}.

Fluorescent molecular sensors with "off–on" switching usually operate on the basis of photoinduced electron-transfer reaction; they are designed as luminophore–spacer–receptor systems[1c,2a] or supramolecular donor–acceptor complexes.[9] Fluorescent probes with cation-triggered emission are barely found among intrinsic fluoroionophores. A rare exception is the fluoroionophore with the donor–acceptor–donor structure reported by Rurack et al.[10] According to the authors, the complexation of this compound with Ca^{2+} entails pronounced fluorescence enhancement (FEF of about 30). For the complex of dye **5** with Ba^{2+}, the FEF value reaches 61, the fluorescence quantum yield being about 0.1, which is a sufficiently high value from the practical standpoint. This result indicates that the potential of intrinsic fluoroionophores for the design of off–on switches has not been exhausted as of yet.

The cation-triggered emission observed for dyes **1a**,**b**, **2b**, **3**, and **5** can be interpreted in terms of the twisted internal charge-transfer (TICT) excited state.[11] For styryl dyes, there exist several possible routes of nonradiative decay of the excited state. These include rotation around the central C=C bond, resulting in *E*–*Z* isomerization,[12] or rotation around one or two single bonds in the C—C=C—C fragment, leading to a nonemissive or weakly emissive TICT state with a high charge-transfer character, which returns to the ground state without geometric isomerization. The absorption spectra of **1a**,**b**, **2b**, **3**, and **5** in MeCN did not change upon long-term visible light irradiation of solutions. In the absence of *E*–*Z* photoisomerization, fast occupation of the nonradiative TICT state is the most probable reason for quenching of the fluorescence of these styryl dyes. This assumption is confirmed by quantum chemical calculations, which showed that the transition of the excited molecule of dye **5** to the TICT state is almost barrier-free.[13] Then the cation-induced enhancement of the fluorescence of dyes **1a**,**b**, **2b**, **3**, and **5** is due to the fact that the metal cation bound to the aza-crown-ether moiety hampers transition of the dye molecule to the TICT state.

It was found that complexation not only leads to fluorescence enhancement but also promotes *E*–*Z* photoisomerization of

dx.doi.org/10.1021/jo401555a | J. Org. Chem. 2013, 78, 9834–9847

dyes **1a,b**, **2b**, **3**, and **5**. The photoirradiation of alkaline-earth metal complexes in MeCN induced changes in the absorption spectra (see Figures S62 and S63 in the Supporting Information) typical of the reversible *E*−*Z* photoisomerization of styryl dyes.[14] In the case of **2b**·M^{2+}, **3**·M^{2+}, and **5**·M^{2+}, the percentage of the *Z* isomer in the *E*−*Z* photostationary equilibrium was quite small due to the low quantum yield of forward *E*−*Z* photoisomerization. The effect of complexation on the photoisomerization of styryl dyes **1a,b** containing a benzothiazole residue proved to be much more pronounced (see Table 3).

Table 3. Data on the Reversible *E*−*Z* Photoisomerization for 1a,b, Protonated Dye 1a, and Complexes 1a·Mg^{2+} and 1a,b·Ca^{2+} [a]

			α_Z,[d] %			
compound	φ_{E-Z}[b]	φ_{Z-E}[c]	313 nm	365 nm	405 nm	436 nm
1a			0	0	0	0
1a·H^+	0.50	0.36	43	88	95	
1a·Mg^{2+}	0.53	0.43	47	81	90	
1a·Ca^{2+}	0.17	0.43		50		66
1b			0	0	0	0
1b·Ca^{2+}			13	38		59

[a]In MeCN (water content < 0.03% v/v) at 23 ± 2 °C. [b]Quantum yield of forward *E*−*Z* photoisomerization. [c]Quantum yield of reverse *Z*−*E* photoisomerization. [d]Percentage of *Z* isomer at the photostationary equilibrium attained upon irradiation with light of the indicated wavelength.

For the complex **1a**·Mg^{2+} and protonated dye **1a**, the *E*−*Z* photoisomerization becomes the key channel of the nonradiative decay from the excited state. The *E*−*Z* photoisomerization quantum yield is 3 times lower for **1a**·Ca^{2+} than for **1a**·Mg^{2+}. In the case of **1b**·Ca^{2+}, *E*−*Z* photoisomerization seems to be even less effective. The lower efficiency of this photoreaction in Ca^{2+} complexes may be caused by the photoinduced re-coordination of Ca^{2+}, which lowers the barrier to the TICT state.

^{1}H NMR Spectroscopy Studies. The conformational behavior of free dyes **1**−**6** and their complexes with group 1 and group 2 metal cations and ethylammonium ions was studied using 2D COSY and NOESY spectra. When analyzing the spectra, we focused on the interactions in the vicinity of the macrocycle nitrogen atom. The NOESY spectra of all dyes containing an *N*-methylbenzoaza-18-crown-6-ether moiety reflected the strong interaction of the benzene ortho proton with the methyl protons and weaker interaction with the protons of the macrocycle *N*-methylene group (Scheme 4, interactions (1) and (2); see Figures S30−S33 in the Supporting Information). In the case of dyes **1a**, **2a**, and **4a** having a 15-membered macrocycle, interaction (2) is weak if at all present (see Figure S29 in the Supporting Information). This means that in solutions, all dyes exist predominantly in the conformations in which the methyl group occurs approximately in the benzene ring plane and the *N*-methylene group deviates considerably from this plane. According to strong interactions (4), the CH_2OAr group is arranged in all dyes approximately in the plane of the benzene ring. These structural features were confirmed by an X-ray diffraction study of dyes **2a** and **4a** (see below).

The ^{1}H NMR signals of dyes in MeCN-d_3 experienced substantial shifts ($\Delta\delta_H$) when alkali or alkaline-earth metal perchlorates or ethylammonium perchlorate were added to solutions. The greatest $\Delta\delta_H$ values were observed for the proton signals of the benzoaza-crown-ether moiety, indicating the formation of host−guest type complexes (Scheme 4). Among the aromatic and unsaturated protons, the greatest downfield shift $\Delta\delta_H$ (up to 0.40 ppm) was found for the proton located in the ortho position to the macrocycle nitrogen. This fact attests to strong interaction between the nitrogen lone electron pair (LEP) and the metal cation located in the macrocycle cavity. This interaction is also responsible for large cation-induced hypsochromic shifts in the absorption spectra of the dyes.

Scheme 4. Complex Formation of Dyes 1b, 2b, 3, 5.[a]

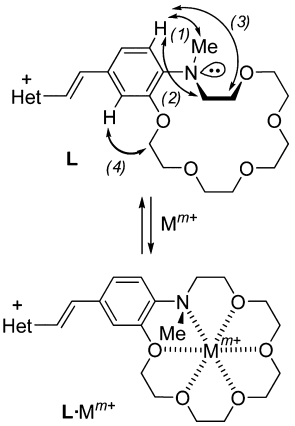

[a]M^{m+} is metal cation or ethylammonium ion (*m* = 1, 2). NOESY interactions between protons near the N atom of the benzoaza-crown-ether moiety are shown by arrows.

Upon the complexation of dyes containing an 18-membered macrocycle with metal cations, interactions (2) in the NOESY spectra are markedly enhanced and interactions (1) are weakened (see Figures S36−S38 in the Supporting Information). In addition, in the case of doubly charged cations, weak interactions (3) are manifested. Probably, upon complexation, the ArN(Me)R moiety rotates around the Ar−N bond, resulting in the expansion of the macrocycle cavity for better binding of the metal cation. As a consequence, the protons of the *N*-methylene group and the ortho proton of the benzene ring approach each other. This conformation of the macrocycle was found previously in the crystalline complex **7b**·Ba$(ClO_4)_2$.[5c]

The conformations of 15-membered macroheterocycles of dyes **1a** and **2a** change little in the presence of metal cations (see Figure S35 in the Supporting Information), probably due to the smaller conformational flexibility of the 15-membered ring compared with the 18-membered ring. Earlier, we found equally slight conformational changes in the studies of crystalline complexes of *N*-methybenzoaza-15-crown-5-ether derivatives with barium cations.[5b,c]

The stability constants of the dye complexes with metal and ethylammonium cations were measured by direct ^{1}H NMR titration in MeCN-d_3. The log *K* values for 1(L):1(M^{m+}) complexes and for the 2(**1a**):1(Ba^{2+}) complex are summarized in Table 4. The stability constants for the 1:1 complexes of **1b**, **2b**, **3**, and **5** with Ca^{2+} and Ba^{2+} were found to be above the upper limit of the measurement range (i.e., the log*K* values for these complexes are higher than 5).

dx.doi.org/10.1021/jo401555a | J. Org. Chem. 2013, 78, 9834−9847

Table 4. Stability Constants for Complexes of Dyes 1a,b, 2b, 3, 5, and 6 with Metal Perchlorates and Ethylammonium Perchlorate, As Measured by ^{1}H NMR Titration[a]

	logK_1 (log K_2)						
compound	$EtNH_3^+$	Li^+	Na^+	K^+	Mg^{2+}	Ca^{2+}	Ba^{2+}
1a	1.4	3.3	2.6	2.0		3.9	>5 (3.6)
1b	3.0	1.8	3.1	3.5	0.9	>5	>5
2b	3.8	2.2	3.5	3.8	1.1	>5	>5
3	3.9	2.5	3.3	3.2	1.5	>5	>5
5	3.8	2.4	3.5	3.2	1.3	>5	>5
6	0.8	1.6	2.6	2.6	1.7	3.5	3.7

[a]MeCN-d_3, 30 ± 1 °C; K_1 = [L·M^{m+}]/([L]·[M^{m+}]), M^{-1}; K_2 = [L_2·M^{m+}]/([L]·[L·M^{m+}]), M^{-1}; the stability constants are measured to within ±30%.

The log K_1 values determined by ^{1}H NMR titration are somewhat lower than the corresponding values obtained by spectrophotometry (cf. data in Table 2) due to the higher water content in MeCN-d_3; however, the principal trends of their variation depending on the nature of the metal cation are retained.

X-ray Diffraction Studies. We were able to grow single crystals of dyes **2a**, **4a,b**, and **5**, and complexes **1a**·$LiClO_4$, **1a**·$Ba(ClO_4)_2$, **2b**·$LiClO_4$, **2b**·$NaClO_4$, and **2b**·$KClO_4$, as suitable for X-ray diffraction analysis. The structures of these compounds are shown in Figures 5 and 6; selected geometric parameters are given in Table 5.

The ethylene bonds in all of the structures are substantially localized (cf. the bond lengths in the C_{Het}—CH═CH—C_{Ar} fragment, Table 5), but the chromophore moieties are nearly planar (the dihedral angle Het/C_6H_3 < 15°), which suggests a high degree of π-conjugation in the Het—C═C—Ar fragment. The bond angles at the macrocycle O(1) atom are close to the perfect sp^2 state value of 120°, and the torsion angles C_{Ar}—C_{Ar}—O(1)—CH_2 are rather small, which is favorable for the conjugation of the O(1) LEP with the π-system of the benzene ring.

The conformations of 15-membered aza macrocycles in **2a** and in both independent molecules **4a** are almost identical and comparable with the conformations previously found for the formyl derivative **7a** and related compounds.[5b,c] The degree of pyramidality of the N(2) atom in **2a** and **4a** (ψ < 12°) rather attests to sp^2 hybridization of this atom, which is favorable for the conjugation of its LEP with the chromophore system. A typical feature of **2a**, **4a**, and all the crystalline *N*-methylbenzoaza-15-crown-5 ethers studied previously is that the methyl substituent is located approximately in the benzene ring plane, the torsion angle C_{Ar}—C_{Ar}—N(2)—CH_3 being close to 0°, whereas the *N*-methylene group always deviates substantially from this plane. This conformation of the macrocycle near N(2) is also retained in solution, as shown by NMR studies (see above).

The 18-membered macrocycles in crystalline dyes **4b** and **5** adopt a conformation in which the *N*-methylene group lies in the benzene ring plane, whereas the methyl group deviates considerably from the plane. This conformation corresponds to a minor conformation in solution. This is probably caused by the crystal packing effect on the conformations of **4b** and **5**. The pyramidality of the N(2) atom in 18-membered macrocycles (ψ ~ 15°) implies an intermediate state of this atom between the sp^2 and sp^3 hybrid states.

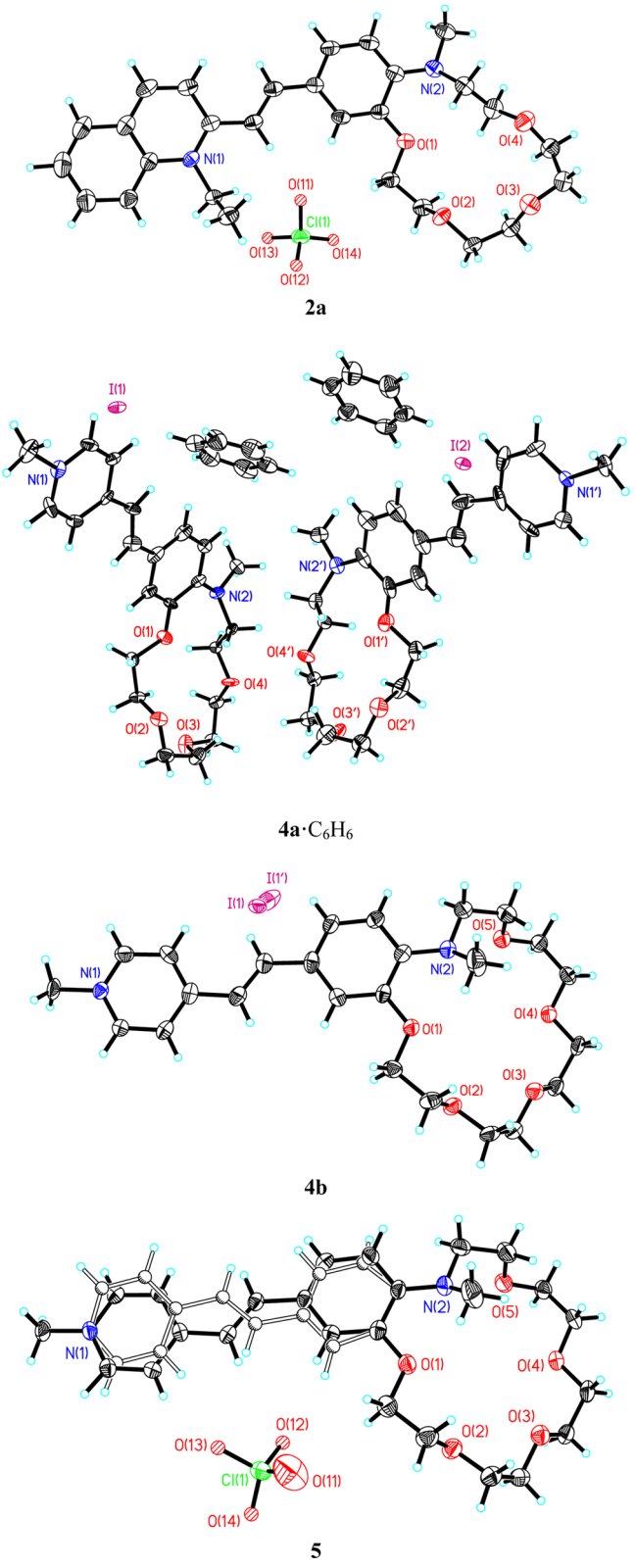

Figure 5. Structures of compounds **2a**, **4a**·C_6H_6 (two independent dye molecules), **4b**, and **5** (two conformers). Thermal ellipsoids are drawn at the 50% probability level. Minor positions of the disordered perchlorate anions in **2a** and **5** are not shown for clarity.

Generally, the conformations of both 15- and 18-membered aza macrocycles are largely preorganized toward the formation of inclusion complexes with metal cations, as the LEPs of the

dx.doi.org/10.1021/jo401555a | J. Org. Chem. 2013, 78, 9834−9847

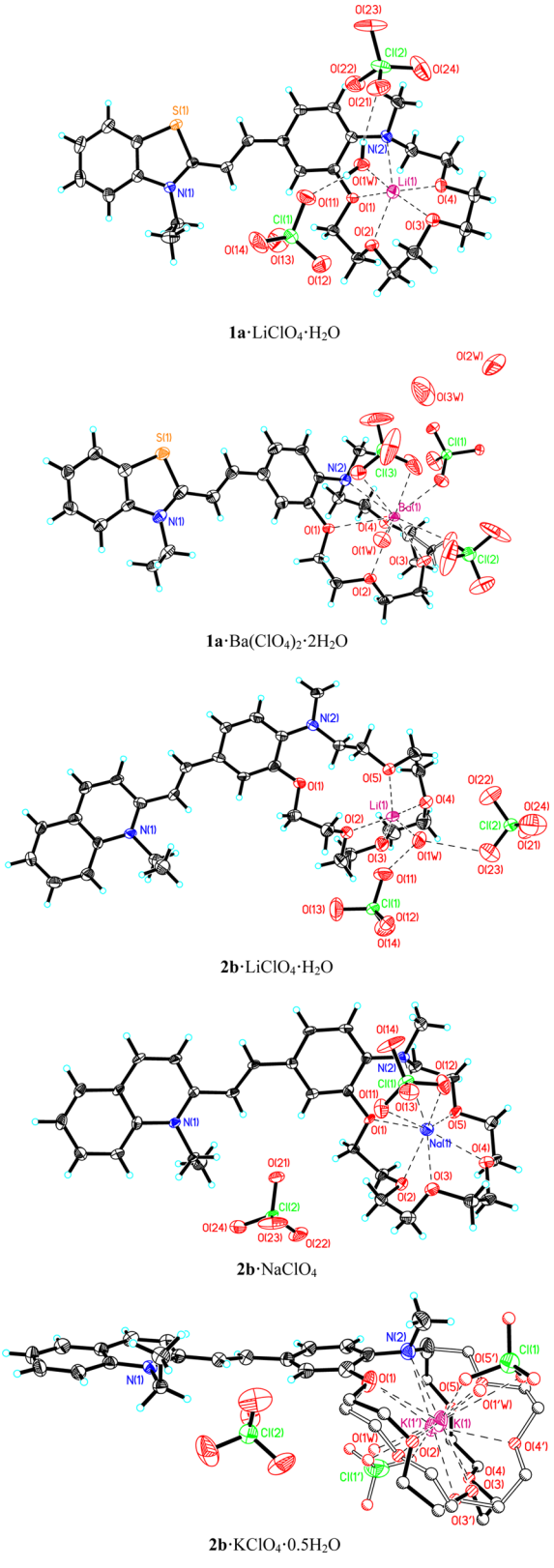

Figure 6. Structures of complexes **1a**·$LiClO_4$·H_2O, **1a**·$Ba(ClO_4)_2$·$2H_2O$, **2b**·$LiClO_4$·H_2O, **2b**·$NaClO_4$, and **2b**·$KClO_4$·$0.5H_2O$ (two conformers). Thermal ellipsoids are drawn at the 40% probability level for **1a**·$Ba(ClO_4)_2$·$2H_2O$ and 50% for other complexes. Minor positions of the disordered $Cl(2)O_4^-$ ion in **2b**·$NaClO_4$ and the crown-ether hydrogen atoms in **2b**·$KClO_4$·$0.5H_2O$ are not shown for clarity. Coordination bonds and hydrogen bonds are shown with dash lines.

N(2) atom and of most oxygen atoms are directed toward the center of the macrocyclic cavity where the guest will be accommodated.

The complexation of dye **1a** with Li^+ or Ba^{2+} does not induce significant conformational rearrangement of the 15-membered azamacrocycle near the benzene ring, as shown by comparison with dyes **2a** and **4a**. This supports the above conclusion about the preorganization of these benzoaza-crown ethers toward binding of metal cations. The small lithium cation is more deeply immersed into the macrocycle cavity of **1a** compared to the large barium cation; the deviations from the mean plane that passes through all macrocycle heteroatoms are 0.56 and 1.69 Å, respectively. Considering the van der Waals radii of the O and N atoms (~1.4 and 1.5 Å), the Ba^{2+} ion is coordinated to approximately the same extent by all heteroatoms of the 15-membered macrocycle: the O(1,2,3,4)···Ba^{2+} and N(2)···Ba^{2+} distances are similar (see Table 5). In the Li^+ complex of **1a**, the O(2,3,4) oxygen atoms far removed from the benzene ring are most involved in binding, whereas the N(2)···Li^+ bond is considerably weakened.

The crystalline complexes of dye **2b** with Li, Na, and K perchlorates can be used to follow the changes in the coordination of alkali metal cations to 18-membered aza macrocycles as a function of the cation size. Despite the low accuracy of determination of the structure of **2b**·$LiClO_4$·H_2O, the geometric characteristics that were found clearly indicated that the macrocycle conformation near the N(2) atom is similar to the conformations of 15-membered benzoaza-crown-ether derivatives and their metal complexes. Undoubtedly, this situation arises due to the large distance of N(2) and O(1) from Li(1), which is coordinated by only O(2,3,4,5) atoms of the macrocycle and by the O(1W) atom of the solvate water molecule. On the comparison of the structures of **2b**·$LiClO_4$·H_2O and **1a**·$LiClO_4$·H_2O, one can conclude that effective binding of the small Li^+ ion requires the presence of 5 heteroatoms, preferably oxygen atoms, in the coordination sphere. Apparently, owing to the limited conformational mobility of the macrocycle, the situation where all heteroatoms of the macrocycle have approached the lithium cation to a distance of ~2.0−2.2 Å is unfavorable.

A similar situation was found for the complex of dye **2b** with $NaClO_4$. The sodium cation forms strong coordination bonds with five oxygen atoms of the 18-membered macrocycle and with two oxygen atoms of the $Cl(1)O_4^-$ anion, whereas the N(2)···Na^+ bond is much longer. This confirms the ability of relatively small metal cations to undergo re-coordination in the macrocycle cavity of *N*-methylaza-crown-ether styryl dyes.

The macrocycle conformations in complexes **2b**·Li^+ and **2b**·Na^+ differ considerably from those in **4b**, **5**, and the previously studied complex **7b**·Ba^{2+}.[5c] In **2b**·Li^+ and **2b**·Na^+, the deviation of the methyl group from the benzene ring plane substantially decreases and the analogous deviation of the *N*-methylene group, conversely, increases considerably. This narrows down the macrocycle cavity, and the relatively small lithium cation deviates from the mean plane through all macrocycle heteroatoms by more than 0.74 Å (i.e., the deviation is even greater than that for the larger potassium cation in complex **2b**·K^+) (see Table 5).

In complex **2b**·$KClO_4$·$0.5H_2O$, the macrocycle is disordered over two predominant conformations of the polyether chain; correspondingly, the positions of the metal cation, $Cl(1)O_4^-$ anion, and the solvent water molecule O(1W) coordinated to the K(1) cation on different sides of the medium plane of the

dx.doi.org/10.1021/jo401555a | J. Org. Chem. 2013, 78, 9834−9847

Table 5. Selected Geometric Parameters for Dyes 2a, 4a·C_6H_6, 4b, and 5 and Complexes 1a·$LiClO_4$·H_2O, 1a·$Ba(ClO_4)_2$·$2H_2O$, 2b·$LiClO_4$·H_2O, 2b·$NaClO_4$, and 2b·$KClO_4$·$0.5H_2O$

bond	2a	4a·C_6H_6[a]	4b	5[b]	1a·$LiClO_4$·H_2O	1a·$Ba(ClO_4)_2$·$2H_2O$	2b·$LiClO_4$·H_2O	2b·$NaClO_4$	2b·$KClO_4$·$0.5H_2O$[b]
					Bond Length, Å				
C_{Het}—CH	1.444(4)	1.447(18); 1.56(3)	1.478(6)	1.457(5); 1.460(19)	1.434(2)	1.440(15)	1.46(2)	1.467(8)	1.457(5)
C_{Ar}—CH	1.440(4)	1.490(13); 1.56(2)	1.463(6)	1.469(5); 1.464(19)	1.452(2)	1.446(15)	1.47(2)	1.447(8)	1.458(5)
HC═CH	1.355(4)	1.334(17); 1.27(2)	1.340(7)	1.330(6); 1.319(19)	1.348(2)	1.336(15)	1.33(2)	1.343(8)	1.355(5)
N(2)···M^{m+}					2.604(3)	3.007(8)	5.13(3)	3.082(5)	2.926(11); 2.931(12)
O(1)···M^{m+}					2.344(3)	2.843(7)	4.25(3)	2.600(4)	2.892(9); 2.842(11)
O(2,3,4,5)···M^{m+}					2.028(3)−2.176(3)	2.766(7)−2.838(6)	2.00(3)−2.14(3)	2.409(5)−2.598(5)	2.646(11)−2.831(10)
O(1W)···M^{m+}					1.945(4)	2.831(8)	1.94(3)		2.85(3); 2.76(3)
					Bond Angle, deg				
C_{Ar}—O(1)—CH_2	117.6(2)	119.5(9); 119.3(10)	117.9(4)	117.2(3)	116.3(1)	120.1(8)	119.7(13)	117.1(4)	118.7(5); 112.4(6)
ψ[c]	11.7(2)	7.3(8); 6.3(10)	15.2(4)	15.1(3)	20.9(1)	23.0(8)	6.2(13)	19.3(5)	20.2(3)
					Torsion Angle, deg				
C_{Ar}—C_{Ar}—N(2)—CH_2	130.4	136.7; −141.4	−6.8	−8.1; −0.4	−105.5	−108.4	−145.5	−119.4	−15.9
C_{Ar}—C_{Ar}—N(2)—CH_3	−10.0	−11.2; 9.3	128.6	127.4; 135.1	24.0	19.2	4.1	11.1	114.0
C_{Ar}—C_{Ar}—O(1)—CH_2	9.4	11.8; −11.5	−4.2	−5.7; −4.2	−9.0	3.4	5.6	21.4	4.2; 17.9
					Dihedral Angle, deg				
Het/C_6H_3	4.7	3.7; 5.2	5.8	3.9; 10.4	14.3	12.4	8.7	4.4	6.4
χ[d]					0.56	1.69	0.73	0.77	0.36; 0.51

[a]For two independent molecules. [b]For two conformations. [c]Pyramidality of atom N(2) (360° minus the sum of bond angles at N(2)). [d]Deviation of the metal cation from the mean plane passing through all heteroatoms of the macrocycle (Å).

dx.doi.org/10.1021/jo401555a | J. Org. Chem. 2013, 78, 9834−9847

macrocycle are disordered. The cation coordination in two conformers is similar: the cation is equatorially surrounded by all heteroatoms of the macrocycle and is positioned approximately at the center of the macrocycle cavity. The distances found, O(1,2,3,4,5)···K^+ and N(2)···K^+, imply approximately the same degree of involvement of all heteroatoms in binding of the relatively large K^+ ion.

The pyramidality of the macrocycle N(2) atom in all complexes, except for **2b**·$LiClO_4$·H_2O, is increased as compared with free dyes. This means that the contribution of the sp^3 hybrid state of this atom, increases upon complexation and, hence, the conjugation of its LEP with the chromophore system deteriorates. This feature is due to a relatively strong N(2)···M^{m+} interaction, which is also responsible for the great ionochromic effects exhibited by styryl dyes **1**−**5** (see above).

CONCLUSIONS

The newly synthesized *N*-methylbenzoaza-crown-containing benzothiazole, pyridine, and quinoline styryl dyes demonstrate high performance as optical molecular sensors for alkali and alkaline-earth metal cations. They greatly surpass analogous intrinsic chromoionophores based on phenylaza-crown ethers both in the magnitude of the ionochromic effect and in the complexing ability. In addition, they function as fluorescent sensors for alkaline-earth metal cations by demonstrating cation-triggered emission. The enhanced characteristics of these chromo(fluoro)ionophores are caused by two factors: higher electron-donating ability of the nitrogen atom in benzoaza-crown-ether moiety and better preorganization of the macrocyclic moiety toward complex formation with cations.

EXPERIMENTAL SECTION

General Methods. The ^1H and ^{13}C NMR spectra were recorded in DMSO-d_6 or MeCN-d_3 at 25−30 °C using the solvent as internal reference (δ_H 2.50 and δ_C 39.43 for DMSO-d_6; δ_H 1.96 for MeCN-d_3). ^1H−^1H COSY, and NOESY spectra and ^1H−^{13}C COSY spectra (HSQC and HMBC) were used to assign the proton and carbon signals; the mixing time in the NOESY experiment was 300 μs. $Mg(ClO_4)_2$, $Ca(ClO_4)_2$, $Sr(ClO_4)_2$, and $Ba(ClO_4)_2$ were dried in vacuo at 230 °C and $LiClO_4$ and $NaClO_4$ were dried in vacuo at 170 °C. $EtNH_3ClO_4$ was obtained by neutralization of ethylamine (70%, aq) with $HClO_4$ (70%, aq) and then dried in vacuo at 60 °C.

Synthesis of Dyes 1−6 (General Method). A mixture of quaternary salt **8**−**12** (0.1 mmol), *N*-methyl(formylbenzo)aza-crown ether **7a,b**[5a,c] or *N*-(formylphenyl)aza-18-crown-6 ether **13**[6] (0.12 mmol), pyridine (30 μL) (in the case of **1** and **6**), piperidine (30 μL) (in the case of **4a**) or pyrrolidine (30 μL) (in the other cases), and MeOH (5 mL) (in the case of **4a**) or abs EtOH (5 mL) (in the other cases) was heated at 85 °C (oil bath) under an argon stream for 10−14 h (in the case of **1**−**3**, **5**, and **6**) or 25 h (in the case of **4a,b**). In the cases of **1**−**3**, **5**, and **6**, the reaction mixture was cooled to −10 °C, and the precipitate that formed was filtered, washed with cold abs EtOH (4 × 2 mL), and dried in air. In the case of **4a,b**, the reaction mixture was thoroughly evaporated in vacuo, and the solid residue was extracted with boiling benzene (4 × 8 mL) and then dried in air. Perchlorates **1a,b**, **2a,b**, **3**, and **5** are nonexplosive substances.

*3-Ethyl-2-[(E)-2-(13-methyl-2,3,5,6,8,9,12,13-octahydro-11H-1,4,7,10,13-benzotetraoxazacyclopentadecin-16-yl)vinyl]-1,3-benzothiazol-3-ium Perchlorate (**1a**).* A dark-red powder (51 mg, 89% yield): mp 194−196 °C; ^1H NMR (500.13 MHz, DMSO-d_6) δ 1.46 (t, ^3J = 7.3 Hz, 3H, *Me*CH_2), 2.95 (s, 3H, MeN), 3.43 (t, ^3J = 7.3 Hz, 2H, CH_2CH_2N), 3.59 (s, 4H, 2 CH_2O), 3.63 (m, 4H, 2 CH_2O), 3.86 (t, ^3J = 7.3 Hz, 2H, CH_2CH_2N), 3.87 (m, 2H, CH_2CH_2OAr), 4.24 (m, 2H, CH_2OAr), 4.90 (q, ^3J = 7.3 Hz, 2H, CH_2N^+), 6.91 (d, ^3J = 8.6 Hz, 1H, 14-H), 7.55 (d, ^4J = 1.8 Hz, 1H, 17-H), 7.57 (dd, ^3J = 8.6 Hz, ^4J = 1.8 Hz, 1H, 15-H), 7.70 (d, ^3J = 15.4 Hz, 1H, CH═C*H*Het), 7.73 (m, 1H, 6-H), 7.82 (m, 1H, 5-H), 8.10 (d, ^3J = 15.4 Hz, 1H, *CH*═CHHet), 8.19 (d, ^3J = 8.6 Hz, 1H, 4-H), 8.35 (d, ^3J = 7.7 Hz, 1H, 7-H) ppm; ^{13}C NMR (125.76 MHz, DMSO-d_6) δ 13.9 (*Me*CH_2), 39.8 (MeN), 43.7 (CH_2N^+), 54.3 (CH_2CH_2N), 68.2 (CH_2OAr), 68.4 (CH_2O), 68.6 (CH_2O), 68.9 (CH_2O), 68.9 (CH_2O), 69.1 (CH_2O), 70.1 (CH_2O), 107.8 (CH═*C*HHet), 112.2 (17-C), 115.6 (14-C), 115.9 (4-C), 124.0 (7-C), 125.0 (16-C), 126.6 (15-C), 127.5 (7a-C), 127.7 (6-C), 129.1 (5-C), 140.8 (3a-C), 146.5 (13a-C), 149.2 (17a-C), 150.1 (*C*H═CHHet), 171.0 (2-C) ppm; UV−vis (MeCN) λ_{max} (ε) = 518 nm (42 000 M^{-1} cm^{-1}); fluorescence (MeCN) λ_{ex} = 450 nm; λ^f_{max} = 642 nm. Anal. Calcd for $C_{26}H_{33}ClN_2O_8S$: C 54.88, H 5.85, N 4.92. Found: C 54.74, H 5.79, N 4.81.

*3-Ethyl-2-[(E)-2-(16-methyl-2,3,5,6,8,9,11,12,15,16-decahydro-14H-1,4,7,10,13,16-benzopentaoxazacyclooctadecin-19-yl)vinyl]-1,3-benzothiazol-3-ium Perchlorate (**1b**).* A dark-red powder (43 mg, 70% yield): mp 186−188 °C; ^1H NMR (500.13 MHz, DMSO-d_6) δ 1.45 (t, ^3J = 7.3 Hz, 3H, *Me*CH_2), 3.02 (s, 3H, MeN), 3.53 (s, 4H, 2 CH_2O), 3.56 (s, 4H, 2 CH_2O), 3.59 (t, ^3J = 5.9 Hz, 2H, CH_2CH_2N), 3.62 (m, 4H, 2 CH_2O), 3.75 (t, ^3J = 5.9 Hz, 2H, CH_2CH_2N), 3.86 (m, 2H, CH_2CH_2OAr), 4.22 (m, 2H, CH_2OAr), 4.90 (q, ^3J = 7.3 Hz, 2H, CH_2N^+), 6.88 (d, ^3J = 8.2 Hz, 1H, 17-H), 7.56 (br s, 1H, 20-H), 7.58 (dd, ^3J = 8.2 Hz, ^4J = 1.8 Hz, 1H, 18-H), 7.69 (d, ^3J = 15.4 Hz, 1H, CH═C*H*Het), 7.72 (m, 1H, 6-H), 7.82 (m, 1H, 5-H), 8.10 (d, ^3J = 15.4 Hz, 1H, *CH*═CHHet), 8.19 (d, ^3J = 8.6 Hz, 1H, 4-H), 8.35 (d, ^3J = 7.7 Hz, 1H, 7-H) ppm; ^{13}C NMR (125.76 MHz, DMSO-d_6) δ 13.8 (*Me*CH_2), 40.7 (MeN), 43.6 (CH_2N^+), 53.9 (CH_2CH_2N), 67.8 (CH_2OAr), 68.7 (CH_2CH_2OAr), 69.2 (CH_2O), 69.7 (CH_2CH_2N, CH_2O), 69.8 (CH_2O), 69.9 (CH_2O), 70.1 (CH_2O), 70.4 (CH_2O), 107.4 (CH═*C*HHet), 112.6 (20-C), 115.6 (17-C), 115.8 (4-C), 123.9 (7-C), 124.5 (19-C), 126.9 (18-C), 127.3 (7a-C), 127.6 (6-C), 129.0 (5-C), 140.7 (3a-C), 146.0 (16a-C), 148.7 (20a-C), 150.0 (CH═CHHet), 170.9 (2-C) ppm; UV−vis (MeCN) λ_{max} (ε) = 526 nm (43 000 M^{-1} cm^{-1}); fluorescence (MeCN) λ_{ex} = 450 nm; λ^f_{max} = 643 nm. Anal. Calcd for $C_{28}H_{37}ClN_2O_9S$: C 54.85, H 6.08, N 4.57. Found: C 54.65, H 6.08, N 4.39.

*1-Ethyl-2-[(E)-2-(13-methyl-2,3,5,6,8,9,12,13-octahydro-11H-1,4,7,10,13-benzotetraoxazacyclopentadecin-16-yl)vinyl]-quinolinium Perchlorate (**2a**).* Dark-violet crystals (32 mg, 57% yield): mp 199−201 °C; ^1H NMR (500.13 MHz, DMSO-d_6) δ 1.55 (t, ^3J = 7.3 Hz, 3H, *Me*CH_2), 2.90 (s, 3H, MeN), 3.35 (t, ^3J = 7.3 Hz, 2H, CH_2CH_2N), 3.59 (s, 4H, 2 CH_2O), 3.63 (m, 4H, 2 CH_2O), 3.88 (t, ^3J = 7.3 Hz, 2H, CH_2CH_2N), 3.89 (m, 2H, CH_2CH_2OAr), 4.24 (m, 2H, CH_2OAr), 5.13 (q, ^3J = 7.3 Hz, 2H, CH_2N^+), 6.92 (d, ^3J = 8.5 Hz, 1H, 14-H), 7.49 (br d, ^3J = 8.5 Hz, 1H, 15-H), 7.50 (br s, 1H, 17-H), 7.57 (d, ^3J = 15.3 Hz, 1H, CH═C*H*Het), 7.90 (m, 1H, 6-H), 8.14 (m, 1H, 7-H), 8.26 (d, ^3J = 15.3 Hz, 1H, *CH*═CHHet), 8.30 (d, ^3J = 7.9 Hz, 1H, 5-H), 8.51 (d, ^3J = 9.2 Hz, 1H, 8-H), 8.54 (d, ^3J = 9.2 Hz, 1H, 3-H), 8.91 (d, ^3J = 9.2 Hz, 1H, 4-H) ppm; ^{13}C NMR (125.76 MHz, DMSO-d_6) δ 13.8 (*Me*CH_2), 39.7 (MeN), 45.8 (CH_2N^+), 54.4 (CH_2CH_2N), 68.0 (CH_2OAr), 68.3 (CH_2CH_2N), 68.6 (CH_2CH_2OAr), 68.8 (CH_2O), 69.0 (CH_2O), 69.1 (CH_2O), 70.1 (CH_2O), 111.6 (17-C), 113.2 (CH═*C*HHet), 115.8 (14-C), 118.6 (8-C), 120.5 (3-C), 125.3 (15-C), 126.2 (16-C), 127.4 (4a-C), 128.4 (6-C), 130.2 (5-C), 134.6 (7-C), 138.0 (8a-C), 142.8 (4-C), 145.6 (13a-C), 148, 9 (*C*H═CHHet), 149.5 (17a-C), 155.2 (2-C) ppm; UV−vis (MeCN) λ_{max} (ε) = 507 nm (37 700 M^{-1} cm^{-1}). Anal. Calcd for $C_{28}H_{35}ClN_2O_8$: C 59.73, H 6.27, N 4.98. Found: C 59.92, H 6.31, N 4.87.

*1-Ethyl-2-[(E)-2-(16-methyl-2,3,5,6,8,9,11,12,15,16-decahydro-14H-1,4,7,10,13,16-benzopentaoxazacyclooctadecin-19-yl)vinyl]-quinolinium Perchlorate (**2b**).* A dark-violet powder (30 mg, 50% yield): mp 184−186 °C; ^1H NMR (500.13 MHz, DMSO-d_6) δ 1.56 (t, ^3J = 7.3 Hz, 3H, *Me*CH_2), 2.98 (s, 3H, MeN), 3.53 (t, ^3J = 5.9 Hz, 2H, CH_2CH_2N), 3.54 (m, 4H, 2 CH_2O), 3.56 (m, 4H, 2 CH_2O), 3.63 (m, 4H, 2 CH_2O), 3.75 (t, ^3J = 5.9 Hz, 2H, CH_2CH_2N), 3.87 (m, 2H, CH_2CH_2OAr), 4.24 (m, 2H, CH_2OAr), 5.12 (q, ^3J = 7.3 Hz, 2H, CH_2N^+), 6.89 (d, ^3J = 8.2 Hz, 1H, 17-H), 7.49 (dd, ^3J = 8.2 Hz, ^4J = 1.8 Hz, 1H, 18-H), 7.50 (br.s, 1H, 20-H), 7.56 (d, ^3J = 15.4 Hz, 1H, CH═C*H*Het), 7.89 (m, 1H, 6-H), 8.13 (m, 1H, 7-H), 8.25 (d, ^3J = 15.4 Hz, 1H, *CH*═CHHet), 8.29 (d, ^3J = 8.0 Hz, 1H, 5-H), 8.49 (d, ^3J

dx.doi.org/10.1021/jo401555a | J. Org. Chem. 2013, 78, 9834−9847

= 9.1 Hz, 1H, 8-H), 8.53 (d, ^3J = 9.1 Hz, 1H, 3-H), 8.89 (d, ^3J = 9.1 Hz, 1H, 4-H) ppm; ^{13}C NMR (125.76 MHz, DMSO-d_6) δ 13.8 ($MeCH_2$), 40.5 (MeN), 45.8 (CH_2N^+), 53.9 (CH_2CH_2N), 67.7 (CH_2OAr), 68.9 (CH_2CH_2OAr), 69.2 (CH_2O), 69.6 (CH_2CH_2N), 69.7 (CH_2O), 69.86 (CH_2O), 69.94 (CH_2O), 70.2 (CH_2O), 70.5 (CH_2O), 112.0 (20-C), 113.1 (CH=CHHet), 116.0 (17-C), 118.6 (8-C), 120.5 (3-C), 125.7 (18-C), 126.0 (19-C), 127.4 (4a-C), 128.3 (6-C), 130.2 (5-C), 134.6 (7-C), 138.0 (8a-C), 142.8 (4-C), 145.3 (16a-C), 148.9 (CH=CHHet), 149.2 (20a-C), 155.3 (2-C) ppm; UV−vis (MeCN) λ_{max} (ε) = 512 nm (32 000 M^{-1} cm^{-1}). Anal. Calcd for $C_{30}H_{39}ClN_2O_9$: C 59.35, H 6.48, N 4.61. Found: C 59.32, H 6.46, N 4.61.

*1-Methyl-4-[(E)-2-(16-methyl-2,3,5,6,8,9,11,12,15,16-decahydro-14H-1,4,7,10,13,16-benzopentaoxazacyclooctadecin-19-yl)vinyl]-quinolinium Perchlorate (**3**).* A dark-violet powder (39 mg, 66% yield): mp 224−225 °C; ^{1}H NMR (500.13 MHz, DMSO-d_6) δ 2.94 (s, 3H, MeN), 3.46 (t, ^3J = 5.9 Hz, 2H, CH_2N), 3.56 (s, 4H, 2 CH_2O), 3.59 (s, 4H, 2 CH_2O), 3.63 (m, 4H, 2 CH_2O), 3.74 (t, ^3J = 5.9 Hz, 2H, CH_2CH_2N), 3.87 (m, 2H, CH_2CH_2OAr), 4.26 (m, 2H, CH_2OAr), 4.48 (s, 3H, MeN^+), 6.88 (d, ^3J = 8.2 Hz, 1H, 17-H), 7.40 (dd, ^3J = 8.2 Hz, ^4J = 1.4 Hz, 1H, 18-H), 7.58 (br s, 1H, 20-H), 8.03 (m, 1H, 6-H), 8.12 (m, 2H, CH=CH), 8.24 (m, 1H, 7-H), 8.38 (m, 2H, 3-H, 8-H), 9.04 (d, ^3J = 8.6 Hz, 1H, 5-H), 9.12 (d, ^3J = 6.4.Hz, 1H, 2-H) ppm; ^{13}C NMR (125.76 MHz, DMSO-d_6) δ 40.3 (MeN), 44.1 (MeN^+), 53.9 (CH_2N), 67.6 (CH_2OAr), 68.9 (CH_2CH_2OAr), 69.3 (CH_2O), 69.6 (CH_2CH_2N), 69.7 (CH_2O), 69.9 (CH_2O), 69.9 (CH_2O), 70.2 (CH_2O), 70.4 (CH_2O), 111.0 (20-C), 114.6 (3-C), 115.2 (CH=CHHet), 116.1 (17-C), 119.0 (8-C), 125.0 (18-C), 125.9 (4a-C), 126.3 (5-C), 126.9 (19-C), 128.7 (6-C), 134.7 (7-C), 138.7 (8a-C), 143.9 (CH=CHHet), 144.5 (16a-C), 147.1 (2-C), 149.4 (20a-C), 152.9 (4-C) ppm; UV−vis (MeCN) λ_{max} (ε) = 519 nm (26 000 M^{-1} cm^{-1}). Anal. Calcd for $C_{29}H_{37}ClN_2O_9$: C 58.73, H 6.29, N 4.72. Found: C 58.75, H 6.31, N 4.64.

*1-Methyl-4-[(E)-2-(13-methyl-2,3,5,6,8,9,12,13-octahydro-11H-1,4,7,10,13-benzotetraoxazacyclopentadecin-16-yl)vinyl]-pyridinium Iodide (**4a**).* A dark-red powder (50 mg, 89% yield): mp 210−212 °C; ^{1}H NMR (500.13 MHz, DMSO-d_6) δ 2.83 (s, 3H, MeN), 3.23 (t, ^3J = 7.2 Hz, 2H, CH_2N), 3.58 (s, 4H, 2 CH_2O), 3.61 (m, 4H, 2 CH_2O), 3.86 (m, 4H, CH_2CH_2N, CH_2CH_2OAr), 4.17 (m, 2H, CH_2OAr), 4.20 (s, 3H, MeN^+), 6.88 (d, ^3J = 8.3 Hz, 1H, 14-H), 7.21 (dd, ^3J = 8.3 Hz, ^4J = 1.3 Hz, 1H, 15-H), 7.29 (d, ^4J = 1.3 Hz, 1H, 17-H), 7.32 (d, ^3J = 16.2 Hz, 1H, CH=CHPy), 7.90 (d, ^3J = 16.2 Hz, 1H, CH=CHPy), 8.08 (d, ^3J = 6.6 Hz, 2H, 3-H, 5-H), 8.74 (d, ^3J = 6.6 Hz, 2H, 2-H, 6-H) ppm; ^{13}C NMR (125.76 MHz, DMSO-d_6) δ 39.4 (MeN), 46.5 (MeN^+), 54.5 (CH_2N), 67.8 (CH_2OAr), 68.2 (CH_2O), 68.6 (CH_2O), 68.7 (CH_2O), 68.9 (2 CH_2O), 70.0 (CH_2O), 110.3 (17-C), 116.2 (14-C), 119.3 (CH=CHPy), 122.4 (3-C, 5-C), 123.2 (15-C), 126.8 (16-C), 141.2 (CH=CHPy), 144.3 (13a-C), 144.4 (2-C, 6-C), 149.9 (17a-C), 152.9 (4-C) ppm; UV−vis (MeCN) λ_{max} (ε) = 456 nm (34 700 M^{-1} cm^{-1}). Anal. Calcd for $C_{23}H_{31}IN_2O_4 \cdot 1.5H_2O$: C 49.92, H 6.19, N 5.06. Found: C 50.18, H 6.29, N 4.95.

*1-Methyl-4-[(E)-2-(16-methyl-2,3,5,6,8,9,11,12,15,16-decahydro-14H-1,4,7,10,13,16-benzopentaoxazacyclooctadecin-19-yl)vinyl]-pyridinium Iodide (**4b**).* A dark-red powder (32 mg, 54% yield): mp 163−164 °C; ^{1}H NMR (500.13 MHz, MeCN-d_3) δ 2.94 (s, 3H, MeN), 3.44 (t, ^3J = 6.1 Hz, 2H, CH_2N), 3.58 (s, 4H, 2 CH_2O), 3.60 (s, 4H, 2 CH_2O), 3.67 (m, 4H, 2 CH_2O), 3.76 (t, ^3J = 6.1 Hz, 2H, CH_2CH_2N), 3.90 (m, 2H, CH_2CH_2OAr), 4.18 (s, 3H, MeN^+), 4.22 (m, 2H, CH_2OAr), 6.90 (d, ^3J = 7.9 Hz, 1H, 17-H), 7.20 (d, ^3J = 15.9 Hz, 1H, CH=CHPy), 7.23 (dd, ^3J = 7.9 Hz, ^4J = 1.8 Hz, 1H, 18-H), 7.25 (d, ^4J = 1.8 Hz, 1H, 20-H), 7.75 (d, ^3J = 15.9 Hz, 1H, CH=CHPy), 7.91 (d, ^3J = 6.7 Hz, 2H, 3-H, 5-H), 8.385 (d, ^3J = 6.7 Hz, 2H, 2-H, 6-H) ppm; ^{13}C NMR (125.76 MHz, DMSO-d_6) δ 40.1 (MeN), 46.4 (MeN^+), 53.8 (CH_2N), 67.4 (CH_2OAr), 68.8 (CH_2CH_2OAr), 69.2 (CH_2O), 69.4 (CH_2CH_2N), 69.6 (CH_2O), 69.8 (2 CH_2O), 70.1 (CH_2O), 70.3 (CH_2O), 110.7 (20-C), 116.3 (17-C), 119.2 (CH=CHPy), 122.4 (3-C, 5-C), 123.4 (18-C), 126.5 (19-C), 141.2 (CH=CHPy), 143.9 (16a-C), 144.4 (2-C, 6-C), 149.5 (20a-C), 152.9 (4-C) ppm; UV−vis (MeCN) λ_{max} (ε) = 456 nm (24 500 M^{-1} cm^{-1}). Anal. Calcd for $C_{25}H_{35}IN_2O_5 \cdot 0.5H_2O$: C 51.82, H 6.26, N 4.83. Found: C 51.66, H 6.02, N 4.78.

*1-Methyl-4-[(E)-2-(16-methyl-2,3,5,6,8,9,11,12,15,16-decahydro-14H-1,4,7,10,13,16-benzopentaoxazacyclooctadecin-19-yl)vinyl]-pyridinium Perchlorate (**5**).* Dark-red crystals (40 mg, 73% yield): mp 191−193 °C; ^{1}H NMR (500.13 MHz, DMSO-d_6) δ 2.89 (s, 3H, MeN), 3.40 (t, ^3J = 5.9 Hz, 2H, CH_2N), 3.53 (s, 4H, 2 CH_2O), 3.55 (s, 4H, 2 CH_2O), 3.62 (m, 4H, 2 CH_2O), 3.71 (t, ^3J = 5.9 Hz, 2H, CH_2CH_2N), 3.84 (m, 2H, CH_2CH_2OAr), 4.17 (m, 2H, CH_2OAr), 4.19 (s, 3H, MeN^+), 6.85 (d, ^3J = 8.2 Hz, 1H, 17-H), 7.21 (dd, ^3J = 8.2 Hz, ^4J = 1.4 Hz, 1H, 18-H), 7.29 (d, ^4J = 1.4 Hz, 1H, 20-H), 7.30 (d, ^3J = 16.4 Hz, 1H, CH=CHPy); 7.89 (d, ^3J = 16.4 Hz, 1H, CH=CHPy), 8.07 (d, ^3J = 6.8 Hz, 2H, 3-H, 5-H), 8.73 (d, ^3J = 6.8 Hz, 2H, 2-H, 6-H) ppm; ^{13}C NMR (125.76 MHz, DMSO-d_6) δ 40.2 (MeN), 46.5 (MeN^+), 53.9 (CH_2N), 67.3 (CH_2OAr), 68.9 (CH_2CH_2OAr), 69.3 (CH_2O), 69.5 (CH_2CH_2N), 69.7 (CH_2O), 69.9 (2 CH_2O), 70.2 (CH_2O), 70.4 (CH_2O), 110.5 (20-C), 116.4 (17-C), 119.2 (CH=CHPy), 122.4 (3-C, 5-C), 123.5 (18-C), 126.6 (19-C), 141.3 (CH=CHPy), 144.0 (16a-C), 144.5 (2-C, 6-C), 149.6 (20a-C), 153.0 (4-C) ppm; UV−vis (MeCN) λ_{max} (ε) = 459 nm (28 000 M^{-1} cm^{-1}); fluorescence (MeCN) λ_{ex} = 430 nm; λ^f_{max} = 666 nm. Anal. Calcd for $C_{25}H_{35}ClN_2O_9$: C 55.30, H 6.50, N 5.16. Found: C 55.39, H 6.58, N 5.18.

*3-Ethyl-2-{(E)-2-[4-(1,4,7,10,13-pentaoxa-16-azacyclooctadecan-16-yl)phenyl]vinyl}-1,3-benzothiazol-3-ium Perchlorate (**6**).* Dark-purple crystals (44 mg, 70% yield): mp 142−144 °C; ^{1}H NMR (500.13 MHz, DMSO-d_6) δ 1.43 (t, ^3J = 7.3 Hz, 3H, $MeCH_2$), 3.54 (s, 12H, 6 CH_2O), 3.58 (m, 4H, 2 CH_2O), 3.66 (m, 4H, 2 CH_2CH_2N), 3.73 (m, 4H, 2 CH_2CH_2N), 4.83 (q, ^3J = 7.3 Hz, 2H, CH_2N^+), 6.89 (d, ^3J = 8.6 Hz, 2H, 3′-H, 5′-H), 7.61 (d, ^3J = 15.3 Hz, 1H, CH=CHHet), 7.68 (m, 1H, 6-H), 7.78 (m, 1H, 5-H), 7.90 (d, ^3J = 8.6 Hz, 2H, 2′-H, 6′-H), 8.08 (d, ^3J = 15.3 Hz, 1H, CH=CHHet), 8.13 (d, ^3J = 8.5 Hz, 1H, 4-H), 8.30 (d, ^3J = 7.9 Hz, 1H, 7-H) ppm; ^{13}C NMR (125.76 MHz, DMSO-d_6) δ 13.7 ($MeCH_2$), 43.4 (CH_2N^+), 50.8 (2 CH_2CH_2N), 67.8 (2 CH_2CH_2N), 69.8 (2 CH_2O), 69.9 (2 CH_2O), 70.0 (4 CH_2O), 105.5 (CH=CHHet), 111.9 (3′-C, 5′-C), 115.6 (4-C), 121.4 (1′-C), 123.9 (7-C), 127.1 (7a-C), 127.4 (6-C), 128.9 (5-C), 133.0 (2′-C, 6′-C), 140.7 (3a-C), 150.4 (CH=CHHet), 152.0 (4′-C), 170.7 (2-C) ppm; UV−vis (MeCN) λ_{max} (ε) = 525 nm (70 000 M^{-1} cm^{-1}). Anal. Calcd for $C_{29}H_{39}ClN_2O_9S$: C 55.54, H 6.27, N 4.47. Found: C 55.24, H 6.26, N 4.25.

Electronic Absorption and Emission Spectroscopy. Experiments were conducted in MeCN (extra pure grade, water content < 0.03% v/v) at 23 ± 2 °C in 1 or 4.75 cm quartz cells with ground-in stoppers. The atmospheric oxygen contained in solutions was not removed. All manipulations with solutions were performed in a darkroom under red light.

Spectrophotometric Titration (SPT). The absorption spectra of the dye−metal cation systems were measured on a range of known dye concentrations (C_L = 2 × 10^{-6} to 4 × 10^{-5} M). In each SPT experiment, the C_L value was maintained constant and the metal cation concentration (C_M) was varied in the range 0−0.003 M (for doubly charged cations) or 0−0.01 M (for singly charged cations). The ionic strength of the solution was maintained at 0.01 M by means of supporting electrolyte Bu_4NClO_4. The complexation stoichiometry, the complex stability constants (K), and the absorption spectra of pure complexes were determined by parametrized matrix modeling of SPT data.[8] In all cases, the SPT data were well approximated by a 1:1 complexation model. For alkaline-earth metal complexes (log K > 7), the stability constants were measured by competitive SPT: the solutions being mixed contained 0.01 M of $NaClO_4$, and the concentration of the alkaline-earth metal salt was varied in the range (0−2) × 10^{-4} M. The parametrized modeling of the competitive SPT data was based on two equilibria:

$$L + M^{2+} \overset{K}{\rightleftarrows} L{\cdot}M^{2+}$$

$$L + Na^{+} \overset{K_{Na}}{\rightleftarrows} L{\cdot}Na^{+}$$

dx.doi.org/10.1021/jo401555a | J. Org. Chem. 2013, 78, 9834−9847

where L is the dye molecule and M^{2+} is the alkaline-earth cation. The equilibrium constant K_{Na} was determined beforehand by direct SPT.

The standard deviation for K in each experiment was <1%. The total measurement error for K is estimated to be about 10% for alkali cations or about 20% for alkaline-earth cations; the relatively high values of the total error are due to possible systematic errors in the C_M and C_L values, and due to possible small variations of the water content in solutions.

Spectrofluorimetry. The fluorescence spectra were corrected taking into account the spectral sensitivity of the photomultiplier tube. The fluorescence quantum yields (φ_f) were determined using the complex $[Ru(bpy)_3]Cl_2$ in water as the standard ($\varphi_f = 0.040$).[15] The formula for calculation of φ_f is

$$\varphi_f = \varphi_{fr}\frac{D_r n^2 A}{D n_r^2 A_r}$$

where all values with subscript r refer to the standard, D is the optical density at the excitation wavelength ($D < 0.1$), n is the refractive index of the solvent, and A is the integrated intensity of the corrected fluorescence spectrum on a cm^{-1} scale.

E–Z Photoisomerization Quantum Yields. Solutions were irradiated by the glass-filtered light of a high-pressure Hg lamp (λ = 313, 365, 405, or 436 nm). The light intensity was measured using a cavity receiver that gave total error in the quantum yield measurements of about 20%. The quantum yields of forward and reverse $E–Z$ photoisomerization (φ_{E-Z} and φ_{Z-E}) were derived from the kinetics of the absorption spectra observed upon steady-state irradiation of a solution of the E isomer at λ = 365 nm. The concentrations of isomers, $C_E(t)$ and $C_Z(t)$, were found by numerical solution of the kinetic equation

$$\frac{dC_E(t)}{dt} = 10^3 I N_A^{-1}[\varphi_{Z-E}\varepsilon_Z C_Z(t) - \varphi_{E-Z}\varepsilon_E C_E(t)]\frac{(1 - 10^{-D(t)})}{D(t)}$$

$$D(t) = [\varepsilon_E C_E(t) + \varepsilon_Z C_Z(t)]l \quad , C_Z(t) = C_L - C_E(t)$$

where I is the light intensity ($cm^{-2}\ s^{-1}$), N_A is the Avogadro number (mol^{-1}), ε_E and ε_Z are the molar absorption coefficients of the isomers at the irradiation wavelength ($M^{-1}\ cm^{-1}$), l is the cell length (cm), and C_L is the total concentration of the styryl dye (M). The absorption spectrum of the pure Z isomer was calculated from the spectra of the $E–Z$ photostationary equilibria that are attained upon irradiation at different wavelengths under the assumption that the $\varphi_{E-Z}/\varphi_{Z-E}$ ratio does not depend on the irradiation wavelength. All calculations were done using parametrized matrix modeling.[8]

^{1}H NMR Titration. MeCN-d_3 (water content < 0.05% v/v) was used as the solvent. The composition and the stability constants of the complexes of dyes with the salts $M^{m+}(ClO_4^-)_m$ were determined by analyzing the shifts of the proton signals of the ligand ($\Delta\delta_H$) depending on the concentration of the added salt. The total concentration of L did not change being equal to $\sim 5 \times 10^{-3}$ M, and the salt concentration was varied starting with zero (the maximum M^{m+}/L ratio was ~3). In the case of titration with $KClO_4$, the total concentration of L was maintained at $\sim 1 \times 10^{-3}$ M due to the limited solubility of the salt. The $\Delta\delta_H$ values were measured to an accuracy of 0.001 ppm. The stability constants of the complexes were calculated by the HYPNMR program.[16]

X-ray Crystal Structure Determinations and Crystal Data. The crystals of dyes and their metal complexes were grown from MeCN solutions, which were slowly saturated with benzene by vapor diffusion method at ambient temperature in the dark. The single crystals of all compounds were coated with perfluorinated oil and mounted on a CCD diffractometer [graphite monochromatized Cu Kα radiation (λ = 1.541 78 Å) for structure **2b**·$LiClO_4$·H_2O and Mo Kα radiation (λ = 0.710 73 Å) for other structures, ω scan mode] under a stream of cold nitrogen (T = 120.0(2) or 170(2) K). The sets of experimental reflections were measured, and the structures were solved by direct methods and refined with anisotropic thermal parameters for all non-hydrogen atoms (except for all oxygen atoms of the disordered perchlorate anion in structure **2a**, for anions I(1′), I(1″), I(2′), and I(2″) in structure **4a**, for the most oxygen atoms of disordered perchlorate anion and carbon atoms of minor conformer in structure **5**, and for the most atoms of disordered macrocyclic fragment in structure **2b**·$KClO_4$·$0.5H_2O$, which were refined isotropically). In most cases, absorption correction was applied using the SADABS method. The hydrogen atoms were fixed at calculated positions at carbon atoms and then refined with an isotropic approximation for **2a** and **1a**·$LiClO_4$·H_2O by using a mixed scheme (an isotropic approximation and a riding model) for **5**, or by using a riding model for other structures. Hydrogen atoms of the solvent water molecule O(1W) in structure **1a**·$LiClO_4$·H_2O were located from the difference Fourier map and refined isotropically. In other hydrated structures, hydrogen atoms of the water molecules were not located.

*Data for **2a**.* $C_{28}H_{35}ClN_2O_8$, M = 563.03, monoclinic, space group $P2_1/n$ (No. 14), dark-red block, a = 10.5263(12) Å, b = 8.2120(10) Å, c = 31.305(4) Å, β = 97.253(2)°, V = 2684.4(5) Å^3, T = 170(2) K, Z = 4, μ = 0.197 mm^{-1}, ρ_{calcd} = 1.393 g cm^{-3}, $2\theta_{max}$ = 58.0°, 25 282 reflections measured, 7139 unique (R_{int} = 0.0845), R_1 = 0.0658 (3495 reflections with $I > 2\sigma(I)$), wR_2 = 0.1663 (all data), goodness-of-fit on F^2 = 0.990, 500 parameters, min/max residual electron density = −0.348/+0.585 e Å^{-3}. The perchlorate anion is disordered over three rotation positions with the occupancy ratio of 0.40:0.30:0.30. SADI command was applied to constrain geometry of this anion.

*Data for **4a**·C_6H_6.* $C_{29}H_{37}IN_2O_4$, M = 604.51, triclinic, space group $P1$ (No. 1), dark-red block, a = 6.536(1) Å, b = 15.092(2) Å, c = 16.092(3) Å, α = 114.521(3)°, β = 99.953(3)°, γ = 93.660(3)°, V = 1406.1(4) Å^3, T = 120.0(2) K, Z = 2, μ = 1.174 mm^{-1} (min/max transmission = 0.7345/0.8344), ρ_{calcd} = 1.428 g cm^{-3}, $2\theta_{max}$ = 54.0°, 7847 reflections measured, 7316 unique (R_{int} = 0.0268), R_1 = 0.0619 (6714 reflections with $I > 2\sigma(I)$), wR_2 = 0.1521 (all data), goodness-of-fit on F^2 = 1.091, 669 parameters, min/max residual electron density = −1.476/+1.507 e Å^{-3}. ISOR command was applied for some atoms. Both independent iodide anions are disordered over three positions with the occupancy ratio of 0.90:0.05:0.05 and 0.90:0.07:0.03.

*Data for **4b**.* $C_{25}H_{35}IN_2O_5$, M = 570.45, triclinic, space group $P\bar{1}$ (No. 2), dark-red block, a = 9.0052(8) Å, b = 10.7537(9) Å, c = 13.4745(12) Å, α = 85.777(3)°, β = 84.127(3)°, γ = 85.136(3)°, V = 1290.56(19) Å^3, T = 120.0(2) K, Z = 2, μ = 1.277 mm^{-1} (min/max transmission = 0.6854/0.8829), ρ_{calcd} = 1.468 g cm^{-3}, $2\theta_{max}$ = 56.0°, 8527 reflections measured, 6034 unique (R_{int} = 0.0294), R_1 = 0.0584 (4474 reflections with $I > 2\sigma(I)$), wR_2 = 0.1713 (all data), goodness-of-fit on F^2 = 1.043, 308 parameters, min/max residual electron density = −0.600/+1.246 e Å^{-3}. The iodide anion is disordered over two close positions with site occupancy ratio of 0.82:0.18. ISOR command was applied for atom I(1′).

*Data for **5**.* $C_{25}H_{35}ClN_2O_9$, M = 543.00, triclinic, space group $P\bar{1}$ (No. 2), red prizm, a = 8.9466(8) Å, b = 10.8772(9) Å, c = 13.6319(12) Å, α = 85.650(5)°, β = 84.387(5)°, γ = 85.205(5)°, V = 1312.5(2) Å^3, T = 120.0(2) K, Z = 2, μ = 0.201 mm^{-1}, ρ_{calcd} = 1.374 g cm^{-3}, $2\theta_{max}$ = 58.0°, 16721 reflections measured, 6936 unique (R_{int} = 0.0796), R_1 = 0.0813 (3079 reflections with $I > 2\sigma(I)$), wR_2 = 0.2245 (all data), goodness-of-fit on F^2 = 0.902, 500 parameters, min/max residual electron density = −0.314/+0.688 e Å^{-3}. Molecular cation of **5** is disordered over two positions with site occupancy ratio of 0.90:0.10. The perchlorate anion reveals rotation disorder over three positions with the occupancy ratio of 0.45:0.35:0.20. SADI command was applied to constrain the geometries of minor conformer of cation and disordered anion.

*Data for **1a**·$LiClO_4$·H_2O.* $C_{26}H_{35}Cl_2LiN_2O_{13}S$, M = 693.46, monoclinic, space group $P2_1/n$ (No. 14), dark-purple prizm, a = 9.0412(3) Å, b = 20.3132(6) Å, c = 17.2983(5) Å, β = 101.284(1)°, V = 3115.52(17) Å^3, T = 120.0(2) K, Z = 4, μ = 0.343 mm^{-1} (min/max transmission =0.8637/0.8807), ρ_{calcd} = 1.478 g cm^{-3}, $2\theta_{max}$ = 58.0°, 25937 reflections measured, 8270 unique (R_{int} = 0.0369), R_1 = 0.0440 (6245 reflections with $I > 2\sigma(I)$), wR_2 = 0.1196 (all data), goodness-of-fit on F^2 = 1.046, 546 parameters, min/max residual electron density = −0.408/+0.623 e Å^{-3}.

*Data for **1a**·$Ba(ClO_4)_2$·$2H_2O$.* $C_{26}H_{37}BaCl_3N_2O_{18}S$, M = 941.33, triclinic, space group $P\bar{1}$ (No. 2), orange plate, a = 8.7392(8) Å, b = 12.4179(11) Å, c = 17.0087(15) Å, α = 75.226(4)°, β = 80.385(4)°, γ

dx.doi.org/10.1021/jo401555a | J. Org. Chem. 2013, 78, 9834–9847

= 84.548(4)°, V = 1757.1(3) Å^3, T = 120.0(2) K, Z = 2, μ = 1.498 mm^{-1} (min/max transmission =0.7340/0.9707), ρ_{calcd} = 1.779 g cm^{-3}, $2\theta_{max}$ = 56.0°, 13507 reflections measured, 8354 unique (R_{int} = 0.1415), R_1 = 0.0885 (4352 reflections with $I > 2\sigma(I)$), wR_2 = 0.2162 (all data), goodness-of-fit on F^2 = 0.916, 479 parameters, min/max residual electron density = −1.970/+1.751 ē Å^{-3}. In molecule **1a**, the C(21)H_2 group of polyether chain is disordered over two positions with the occupancy ratio of 0.76:0.24. ISOR command was applied for some atoms.

Data for ***2b***·*LiClO$_4$·H$_2$O*. $C_{30}H_{41}Cl_2LiN_2O_{14}$, M = 731.49, triclinic, space group $P\bar{1}$ (No. 2), dark-red needle, a = 7.0910(9) Å, b = 14.0438(15) Å, c = 17.133(2) Å, α = 98.366(10)°, β = 93.940(7)°, γ = 94.900(6)°, V = 1676.2(3) Å^3, T = 120.0(2) K, Z = 2, μ = 2.364 mm^{-1} (min/max transmission = 0.7646/0.9767), ρ_{calcd} = 1.449 g cm^{-3}, $2\theta_{max}$ = 100.0°, 5763 reflections measured, 3153 unique (R_{int} = 0.0488), R_1 = 0.1717 (2619 reflections with $I > 2\sigma(I)$), wR_2 = 0.4658 (all data), goodness-of-fit on F^2 = 1.180, 443 parameters, min/max residual electron density = −0.734/+2.039 ē Å^{-3}. The experiment was collected from a very thin-plate crystal and because residual electron densities were relatively high; the highest peaks were located about the oxygen atoms of perchlorate anions at distances smaller than 1.5 Å. ISOR command was applied to oxygen atoms of anion Cl(2)O_4^-.

Data for ***2b***·*NaClO$_4$*. $C_{30}H_{39}Cl_2N_2NaO_{13}$, M = 729.52, triclinic, space group $P\bar{1}$ (No. 2), red prizm, a = 8.3396(6) Å, b = 9.6570(8) Å, c = 21.7107(17) Å, α = 94.045(4)°, β = 99.674(4)°, γ = 100.827(4)°, V = 1683.5(2) Å^3, T = 120.0(2) K, Z = 2, μ = 0.274 mm^{-1} (min/max transmission = 0.8708/0.9079), ρ_{calcd} = 1.439 g cm^{-3}, $2\theta_{max}$ = 55.0°, 9622 reflections measured, 7401 unique (R_{int} = 0.0545), R_1 = 0.1069 (4409 reflections with $I > 2\sigma(I)$), wR_2 = 0.2193 (all data), goodness-of-fit on F^2 = 1.098, 461 parameters, min/max residual electron density = −0.569/+0.419 ē Å^{-3}. Perchlorate anion Cl(2)O_4^- is disordered over two close positions with site occupancy ratio of 0.53:0.47. SADI and ISOR commands were applied to constrain the geometry of this anion.

Data for ***2b***·*KClO$_4$·0.5H$_2$O*. $C_{30}H_{40}Cl_2KN_2O_{13.5}$, M = 754.64, triclinic, space group $P\bar{1}$ (No. 2), red block, a = 8.8035(3) Å, b = 9.5442(3) Å, c = 23.1098(8) Å, α = 90.879(2)°, β = 98.589(2)°, γ = 115.328(2)°, V = 1728.57(10) Å^3, T = 120.0(2) K, Z = 2, μ = 0.376 mm^{-1} (min/max transmission = 0.8197/0.8640), ρ_{calcd} = 1.450 g cm^{-3}, $2\theta_{max}$ = 58.0°, 18589 reflections measured, 8931 unique (R_{int} = 0.0505), R_1 = 0.0964 (4928 reflections with $I > 2\sigma(I)$), wR_2 = 0.3077 (all data), goodness-of-fit on F^2 = 1.074, 493 parameters, min/max residual electron density = −0.683/+1.219 ē Å^{-3}. In this structure, the macrocyclic moiety, the potassium cation, the perchlorate anion Cl(1)O_4^-, and the solvate water molecule O(1W) are distributed over a series of proximate positions, which could not be completely localized; for final refinement, two the most occupied positions with the ratio of 0.52:0.48 were used. The whole occupancy of the water molecule is 0.5. This considerable conformational disorder strongly reduces an accuracy of the X-ray diffraction study. SADI and ISOR commands were applied.

All the calculations were performed using the SHELXTL-Plus software.[17] CCDC 903335 (**2a**), 903336 (**4a**·C_6H_6), 903337 (**4b**), 903338 (**5**), 903339 (**1a**·LiClO$_4$·H$_2$O), 903340 [**1a**·Ba(ClO$_4$)$_2$·2H$_2$O], 903341 (**2b**·LiClO$_4$·H$_2$O), 903342 (**2b**·NaClO$_4$), and 903343 (**2b**·KClO$_4$·0.5H$_2$O) contain supplementary crystallographic data for this paper. These data can be obtained free of charge from the Cambridge Crystallographic Data Center via www.ccdc.cam.ac.uk/data_request/cif.

■ ASSOCIATED CONTENT

Ⓢ Supporting Information

^{1}H and ^{13}C NMR, ^{1}H−^{1}H COSY and NOESY, and ^{1}H−^{13}C COSY (HSQC and HMBC) spectra, absorption and fluorescence spectra, and X-ray crystallographic data (CIF). This material is available free of charge via the Internet at http://pubs.acs.org.

■ AUTHOR INFORMATION

Corresponding Author

*S. P. Gromov. E-mail: spgromov@mail.ru.

Notes

The authors declare no competing financial interest.

■ ACKNOWLEDGMENTS

Financial support from the Russian Foundation for Basic Research, the Russian Academy of Sciences, the Ministry of Education and Science of Russian Federation, the Royal Society of Chemistry (L.G.K.), and the Engineering and Physical Sciences Research Council (EPSRC) for a Senior Research Fellowship (J.A.K.H.) is gratefully acknowledged.

■ REFERENCES

(1) (a) Löhr, H.-G.; Vögtle, F. *Acc. Chem. Res.* **1985**, *18*, 65−72. (b) Hayashita, T.; Takagi, M. In *Comprehensive Supramolecular Chemistry. Vol. 1. Molecular recognition: Receptors for cationic guests*; Gokel, G. W., Ed.; Pergamon: Oxford, U.K., 1996; p 635. (c) de Silva, A. P.; Gunaratne, H. Q. N.; Gunnlaugsson, T.; Huxley, A. J. M.; McCoy, C. P.; Rademacher, J. T.; Rice, T. E. *Chem. Rev.* **1997**, *97*, 1515. (d) Valeur, B.; Leray, I. *Coord. Chem. Rev.* **2000**, *205*, 3. (e) Gokel, G. W.; Leevy, W. M.; Weber, M. E. *Chem. Rev.* **2004**, *104*, 2723. (f) Ushakov, E. N.; Alfimov, M. V.; Gromov, S. P. *Russ. Chem. Rev.* **2008**, *77*, 39. (g) Tsukanov, A. V.; Dubonosov, A. D.; Bren, V. A.; Minkin, V. I. *Chem. Heterocycl. Compd.* **2008**, *44*, 899.

(2) (a) Rurack, K.; Resch-Genger, U. *Chem. Soc. Rev.* **2002**, *31*, 116. (b) Fery-Forgues, S.; Al-Ali, F. *J. Photochem. Photobiol., C* **2004**, *5*, 139.

(3) (a) Izatt, R. M.; Pawlak, K.; Bradshaw, J. S.; Bruening, R. L. *Chem. Rev.* **1991**, *91*, 1721. (b) Ushakov, E. N.; Gromov, S. P.; Fedorova, O. A.; Alfimov, M. V. *Russ. Chem. Bull.* **1997**, *46*, 463.

(4) (a) Mathevet, R.; Jonusauskas, G.; Rullière, C.; Létard, J.-F.; Lapouyade, R. *J. Phys. Chem.* **1995**, *99*, 15709. (b) Rusalov, M. V.; Uzhinov, B. M.; Alfimov, M. V.; Gromov, S. P. *Russ. Chem. Rev.* **2010**, *79*, 1099.

(5) (a) Gromov, S. P.; Dmitrieva, S. N.; Vedernikov, A. I.; Kuz'mina, L. G.; Churakov, A. V.; Strelenko, Yu. A.; Howard, J. A. K. *Eur. J. Org. Chem.* **2003**, 3189. (b) Vedernikov, A. I.; Dmitrieva, S. N.; Kuz'mina, L. G.; Kurchavov, N. A.; Strelenko, Yu. A.; Howard, J. A. K.; Gromov, S. P. *Russ. Chem. Bull., Int. Ed.* **2009**, *58*, 978. (c) Gromov, S. P.; Dmitrieva, S. N.; Vedernikov, A. I.; Kurchavov, N. A.; Kuz'mina, L. G.; Strelenko, Yu. A.; Alfimov, M. V.; Howard, J. A. K. *J. Phys. Org. Chem.* **2009**, *22*, 823.

(6) Dix, J. P.; Vögtle, F. *Chem. Ber.* **1980**, *113*, 457.

(7) Gromov, S. P.; Ushakov, E. N.; Fedorova, O. A.; Soldatenkova, V. A.; Alfimov, M. V. *Russ. Chem. Bull.* **1997**, *46*, 1143.

(8) Ushakov, E. N.; Gromov, S. P.; Fedorova, O. A.; Pershina, Yu. V.; Alfimov, M. V.; Barigelletti, F.; Flamigni, L.; Balzani, V. *J. Phys. Chem. A* **1999**, *103*, 11188.

(9) Vedernikov, A. I.; Ushakov, E. N.; Efremova, A. A.; Kuz'mina, L. G.; Moiseeva, A. A.; Lobova, N. A.; Churakov, A. V.; Strelenko, Yu. A.; Alfimov, M. V.; Howard, J. A. K.; Gromov, S. P. *J. Org. Chem.* **2011**, *76*, 6768.

(10) Rurack, K.; Rettig, W.; Resch-Genger, U. *Chem. Commun.* **2000**, 407.

(11) Grabowski, Z. R.; Rotkiewicz, K.; Rettig, W. *Chem. Rev.* **2003**, *103*, 3899.

(12) Hammond, G. S.; Saltiel, J.; Lamola, A. A.; Turro, N. J.; Bradshaw, J. S.; Cowan, D. O.; Counsell, R. C.; Vogt, V.; Dalton, C. *J. Am. Chem. Soc.* **1964**, *86*, 3197.

(13) Freidzon, A. Ya.; Bagatur'yants, A. A.; Ushakov, E. N.; Gromov, S. P.; Alfimov, M. V. *Int. J. Quantum Chem.* **2011**, *111*, 2649.

(14) Güsten, H.; Schulte-Frohlinde, D. *Chem. Ber.* **1971**, *104*, 402.

(15) Suzuki, K.; Kobayashi, A.; Kaneko, S.; Takehira, K.; Yoshihara, T.; Ishida, H.; Shiina, Y.; Oishi, S.; Tobita, S. *Phys. Chem. Chem. Phys.* **2009**, *11*, 9850.

(16) Frassineti, C.; Ghelli, S.; Gans, P.; Sabatini, A.; Moruzzi, M. S.; Vacca, A. *Anal. Biochem.* **1995**, *231*, 374.
(17) *SHELXTL-Plus*, Version 5.10; Bruker AXS, Inc.: Madison, WI, 1997.